Journal of South American Earth Sciences 127 (2023) 104315

Contents lists available at ScienceDirect

Journal of South American Earth Sciences

journal homepage: www.elsevier.com/locate/jsames

Late Cretaceous calcareous nannofossil assemblages from Colombia: Biostratigraphic contributions to northwestern South American Basins

Estefanía Angulo-Pardo [a,*], Felipe Vallejo-Hincapié [a,b], Rodrigo Do Monte Guerra [c], Andrés Pardo-Trujillo [a], Carlos A. Giraldo-Villegas [a,d], Jenny García González [e], Sebastian Hernández Duran [f], Sergio Herrera Quijano [f], Angelo Plata Torres [a,b], Raúl Trejos-Tamayo [a,b]

[a] Instituto de Investigaciones en Estratigrafía (IIES), Grupo de Investigaciones en Estratigrafía y Vulcanología (GIEV-Cumanday) y Departamento de Ciencias Geológicas de La Universidad de Caldas, Calle 65 # 26-10, Manizales, 1700004, Colombia
[b] Departamento de Geología, Facultad de Ciencias, Universidad de Salamanca, Plaza de Los Caídos, S/n, Salamanca, 37008, Spain
[c] Technological Institute for Paleoceanography and Climate Change (itt Oceaneon), UNISINOS University, São Leopoldo, 93.022–750, Brazil
[d] Departamento de Estratigrafía y Paleontología, Universidad de Granada, Avenida Fuente Nueva S/n, Granada, 18071, Spain
[e] Fundación Universitaria Del Área Andina, Transv 22 Bis #4-105, Valledupar, 200001, Colombia
[f] Departamento de Geociencias, Universidad Nacional de Colombia, Carrera 45 # 26-85, Bogotá, 111321, Colombia

ARTICLE INFO

Keywords:
Micropaleontology
Caribbean nannofossils
La luna sea
Eastern equatorial Pacific nannofossils

ABSTRACT

The Upper Cretaceous deposits of northwestern Colombia accumulated in two regions with distinct tectonic settings. The eastern deposits, consisting of Turonian–Maastrichtian rocks from the Upper Magdalena Valley (UMV) and the Cesar-Rancheria basins, were deposited by an epicontinental sea that partially covered the South American Plate. In contrast, the western deposits, which comprise a series of highly faulted and folded Coniacian–Maastrichtian deposits in the Sinú-San Jacinto Folded Belt (SSJFB), Gorgonilla Island, and Western Cordillera, were influenced by a seaway connecting the eastern Pacific Ocean with the proto-Caribbean Sea and were deposited near the collision zone between the Caribbean and South American Plates. We conducted a biostratigraphic analysis of 119 rock samples from these deposits. Although some well-preserved microfossils were found in the Cesar-Ranchería Basin, most samples exhibited poor to moderate preservation of nannofossils. Biostratigraphic markers identified in the Upper Magdalena Valley Basin were *Quadrum gartneri*, *Micula concava*, *Micula staurophora*, *Lithastrinus septenarius*, *Lithastrinus grillii*, *Arkhangelskiella cymbiformis*, *Uniplanarius trifidus*, *Uniplanarius sissinghii*, and *Reinhardtites anthophorus*. In the Cesar-Rancheria Basin, the markers identified were *Arkhangelskiella cymbiformis*, *Lithraphidites* cf. *L. praequadratus*, and an acme of *Kamptnerius magnificus*. Based on these taxa, the eastern stratigraphic sections accumulated sometime between UC7 (CC11) and UC20 (CC26) biozones, which is equivalent to an age range of early Turonian to upper Maastrichtian. Key biostratigraphic taxa from the western outcrops were more limited, yielding only *Uniplanarius trifidus* and *Uniplanarius sissinghii*, which are indicative of biozones UC15d–UC17 (CC22–CC23). This signifies a sedimentation age sometime from late Campanian to early Maastrichtian. Our results correlate well with previous age models and reveal that undistinguished upper Campanian–lower Maastrichtian deposits of the collision zone can be correlated with the last marine deposits of the epicontinental sea in the UMV. Although calcareous nannofossils from the Cesar-Rancheria Basin displayed the best preservation, low-latitude biostratigraphic markers were absent in this locality, making regional correlations challenging. We hypothesize that these deposits formed during the Maastrichtian, but changes in oceanic water conditions of the proto-Caribbean Sea affected productivity and preservation of biostratigraphic markers.

* Corresponding author.
E-mail address: estefania.angulo@ucaldas.edu.co (E. Angulo-Pardo).

https://doi.org/10.1016/j.jsames.2023.104315
Received 16 November 2022; Received in revised form 15 March 2023; Accepted 20 March 2023
Available online 18 April 2023

1. Introduction

Upper Cretaceous sedimentary deposits from northwestern South America accumulated in contrasting paleoenvironmental and tectonic settings, which can be separated into eastern and western regions (Fig. 1A and B). Marine deposits from the eastern region, including the Upper and Middle Magdalena Valley and Cesar-Rancheria basins, were deposited under shallow marine conditions of an epicontinental sea known as the La Luna Sea (Villamil and Arango, 1998; Villamil, 1998; Erlich et al., 2000; Páez-Reyes et al., 2021). In contrast, the western deposits exposed as deformed belts in the Sinú-San Jacinto Folded Belt (SSJFB), Tumaco and Chocó Basin, and Western Cordillera accumulated in deeper marine environments associated with a seaway between the proto-Caribbean Sea and the eastern equatorial Pacific Ocean (Fig. 1B) (Duque-Caro, 1972a, 1990; Mann, 1999; Iturralde-Vinent, 2005; Kerr and Tarney, 2005; Villagómez et al., 2011; Spikings et al., 2015; Buchs

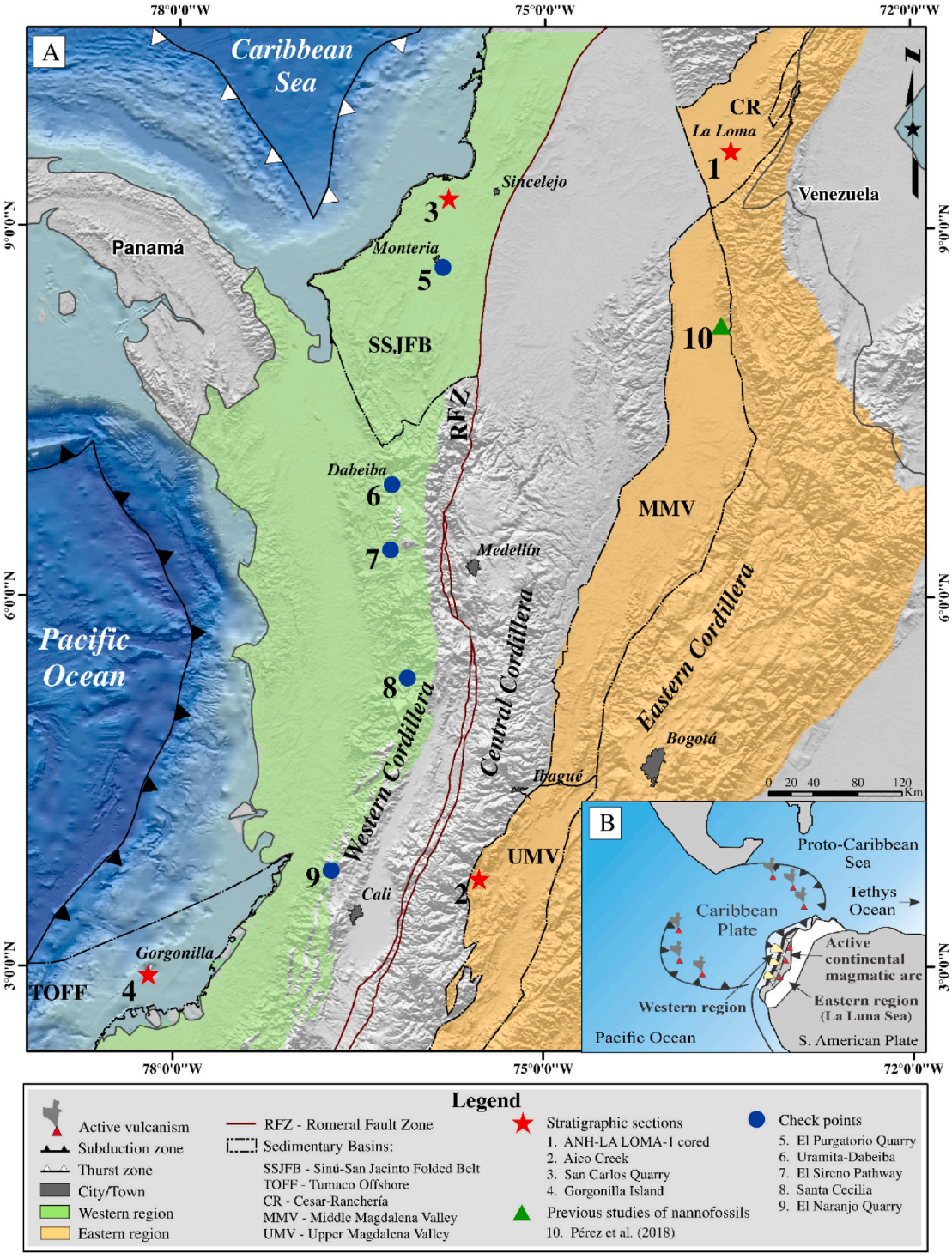

Fig. 1. Geographic location of the western and eastern Upper Cretaceous deposits studied in this research, as well as previous studies related to calcareous nannofossils. **A)** Geographic location of the western and eastern deposits studied here and previous studies concerning calcareous nannofossils. **B)** Paleogeographic reconstruction of northwestern South America during the Late Cretaceous, adapted from Pardo-Trujillo et al. (2020), illustrating the tectonic and paleoenvironmental settings of the different deposits.

et al., 2018; Pardo-Trujillo et al., 2020; Giraldo-Villegas et al., 2023). Our review of the published literature found that Upper Cretaceous deposits from the eastern region yield more detailed chronostratigraphic and lithostratigraphic information than oceanic rocks from the western region (Appendix A) (Bürgl and Dumit, 1954; Gandolfi, 1955; Etayo--Serna et al., 1982; Jaramillo and Yepes, 1994; Guzmán et al., 1994, 2004; Guerrero et al., 2000; Tchegliakova and Mojica, 2001; Yepes, 2001; Martínez, 2003; Patarroyo, 2011; Patarroyo et al., 2017; 2017, 2022; Pérez et al., 2018; Páez-Reyes et al., 2021). Our review also revealed that little is known about the biostratigraphy of calcareous nannofossils, and that nannofossil assemblages were particularly abundant and diverse in deposits formed near the Cenomanian/Turonian boundary (Páez-Reyes et al., 2021) and generally poorly preserved in rocks from the Turonian to the Maastrichtian (De Romero et al., 2003; Pérez et al., 2018; Barrantes et al., 2019; Patiño et al., 2019; Pardo--Trujillo et al., 2020).

Calcareous nannofossils are exclusively marine and planktonic microfossils, which are found in oceanic deposits as old as the Upper Triassic (Bown and Young, 1998). Their wide distribution, high morphological diversity, and high abundance, as well as their calibration in well-dated stratigraphic sections, make them a valuable biostratigraphic proxy for dating and correlating marine deposits on a latitudinal scale (Odin, 2001; Odin and Lamaurelle, 2001; Lamolda et al., 2014; Walaszczyk et al., 2021). Well-documented biogeographic patterns of these microfossils reveal variations between high (>50°N and >40°S) and low latitudes (between 45°N and 10°S) during the Late Cretaceous (Thierstein, 1981; Concheyro, 1995; Watkins et al., 1996; Burnett, 1998; Lees, 2002; Moore, 2016). As a result, different biozonations have been constructed for Upper Cretaceous deposits around the globe; those of Sissingh (1977, 1978), modified by Perch-Nielsen (1985), and Burnett (1998) are the most commonly used for biostratigraphic studies in low-latitude areas. This study aims to use well-calibrated biostratigraphic markers to date and correlate Upper Cretaceous deposits from the eastern and western regions of Colombia, building a chronostratigraphic framework based on nannofossils (Roth, 1978; Bralower et al., 1995).

2. Geological and paleoceanographic context

During the Late Cretaceous, in the eastern region, thick, organic-rich mudrock deposits of the epicontinental La Luna Sea accumulated on the South American Plate between Colombia and Venezuela, forming some of the best hydrocarbon source-rocks from northern South America (Talukdar and Marcano, 1994; Villamil et al., 1999; Mann et al., 2006) (Fig. 1B). The La Luna Sea experienced maximum flooding between the Turonian and Coniacian and subsequently began retreating during the Campanian–Maastrichtian (Villamil and Arango, 1998; Villamil, 1998; Erlich et al., 2000). The sea's retreat was due to tectonic adjustments as the Caribbean Plate collided with the western margin of the South American Plate and to global sea-level fall from the late Campanian to Maastrichtian (Gómez et al., 2003; Villagómez et al., 2011; Villagómez and Spikings, 2013; Haq, 2014; Bayona, 2018; Pardo-Trujillo et al., 2020). According to micropaleontological evidence, oceanic conditions of the La Luna Sea were similar to those described for tropical and subtropical latitudes of the Tethyan Ocean during most of the Late Cretaceous (Petters, 1955; Martínez, 1989; Jaramillo and Yepes, 1994; Yepes, 2001; Dueñas and Gómez, 2013). These conditions were characterized by reduced oxygenation that caused anoxic events near the Cenomanian/Turonian boundary and the Coniacian (Martínez, 2003; Pérez et al., 2018; Páez-Reyes et al., 2021). The La Luna Sea also recorded conditions of upwelling from the Santonian to Maastrichtian (Fabre, 1985; Föllmi et al., 1992; Etayo Serna, 1994; Villamil and Arango, 1998; Villamil, 1998; Erlich et al., 2000; Sarmiento, 2018), coinciding with a global cooling episode in low latitudes (Barrera and Savin, 1999; Linnert et al., 2014; O'Brien et al., 2017) and a change in marine productivity in northern oceanic basins of South America (Yepes, 2001; Martínez, 2003; Patarroyo et al., 2022).

The Late Cretaceous history of the western region is less documented; however, some previous works have characterized turbiditic and hemipelagic deposits accumulated in deep marine environments during the Campanian–Maastrichtian (Duque-Caro, 1972a, 1972b, 1978, 1979, 1984; Duque-Caro and Dueñas, 1987; Clavijo and Barrera, 2001; Guzmán, 2007; Pardo-Trujillo et al., 2020; Giraldo-Villegas et al., 2023). These deposits were deposited over the allochthonous rocks of the Caribbean Plate, which began to block the marine connection between the Pacific Ocean and the Caribbean Sea as it was colliding with the South American Plate during the Late Cretaceous–early Paleogene (Duque-Caro, 1972a, 1990; Mann, 1999; Moreno-Sánchez and Pardo-Trujillo, 2003; Guzmán et al., 2004; Iturralde-Vinent, 2005; Guzmán, 2007; Mora et al., 2017; Buchs et al., 2018; Pardo-Trujillo et al., 2020; Giraldo-Villegas et al., 2023) (Fig. 1B). In the western region, marine sedimentation was largely influenced by volcanic activity from volcanic arcs built on the Caribbean and South American Plates and by erosion of the South American continental margin (Weber et al., 2015; Buchs et al., 2018; Pardo-Trujillo et al., 2020; Zapata-Villada et al., 2017, 2021; Botero-García et al., 2023) (Fig. 1B). In addition, marine deposits from the Gorgonilla Island in the Pacific Ocean show that the Chicxulub bolide impact perturbated sedimentation during the end of the Cretaceous (Bermúdez et al., 2016; Renne et al., 2018). Although the deformation associated with the collision of the Caribbean Plate against the South American margin is still a matter of study, it is thought that complex tectonic interactions caused obduction of a suite of igneous and marine deposits, which are currently exposed along with the western Colombian margin (Western Cordillera, and Gorgonilla Island) and partially buried by Cenozoic sediments in the SSJFB (Duque-Caro, 1972a; Nivia, 1996; Villagómez et al., 2011; Echeverri et al., 2015; Patiño et al., 2019).

3. Lithostratigraphy

3.1. Eastern region

In the eastern region, we extracted calcareous nannofossils from deposits outcropping in the Upper Magdalena Valley (UMV) and Cesar-Rancheria basins. The Aico Creek in the UMV section encompasses the Loma Gorda Formation, Oliní Group (which includes Lidita Inferior, Aico Shale, and Lidita Superior formations), and Buscavida Formation (Hernández, 2021) (Figs. 2 and 3). The Loma Gorda Formation consists of ~23 m of laminated limestones (*mudstones*, *wackestones*, and *packstones*) interlayered with sporadic phosphate deposits (Fig. 2A–I) associated with low-energy marine environments below the storm-wave base (Hernández, 2021). These rocks are overlain by the Lidita Inferior Formation (Fig. 2A–II), which is mainly composed of ~49 m of interlayered laminated limestones (*wackestones*) with cherts. This formation also exhibits laminated mudrocks and phosphatic beds accumulated under low-energy marine environments below the fair-weather wave base. Above this lies a ~23-m-thick deposit informally named the Aico Shale formation (Hernández, 2021), which is stratigraphically equivalent to the El Cobre Formation recognized by Garzon et al. (2012) in neighboring outcrops of the Aico Creek section. This unit consists of laminated claystones deposited under offshore conditions. Overlying these rocks are marine rocks of the Lidita Superior Formation, the last formation of the Oliní Group (Fig. 2A–III). These deposits are characterized by alternating laminated cherts and limestones (*mudstones* and *wackestones*) deposited in offshore marine environments. In the upper part of the stratigraphic section, sedimentary rocks of the Buscavida Formation (Fig. 2A–IV) measure up to ~81 m-thick (Hernández, 2021). This formation consists of laminated limestones (*wackestones, packstones*), mudrocks, sandy siltstones, and fine to very fine-grained sandstones with horizontal and flaser laminations accumulated in offshore and upper shoreface settings.

The ANH-LA LOMA-1 core-stratigraphic section (Fig. 2B), in the

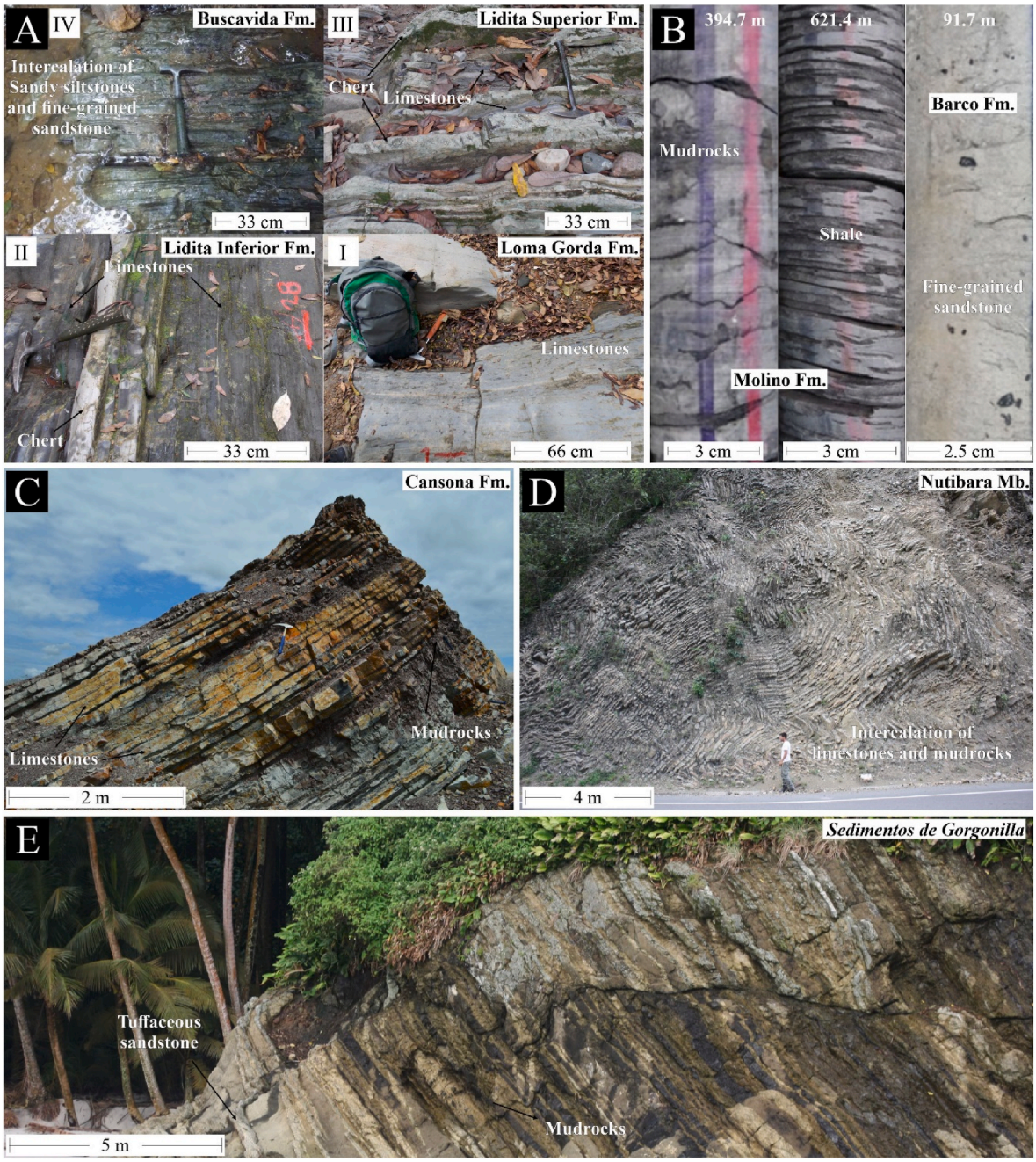

Fig. 2. Photographic record of the studied lithostratigraphic units studied in both the eastern and western regions. In the Eastern region, the Aico Creek section (A) displays four different intervals corresponding to laminated limestone of the Loma Gorda Fm. (I), laminated limestone and cherts of the Lidita Inferior Fm. (II), an alternation between laminated cherts and limestones of the Lidita Superior Fm. (III), and sandy siltstones, and fine to very fine-grained sandstones of the Buscavida Fm. (IV). The ANH-LA LOMA-1 cored-stratigraphic section of the Molino Fm. (B) Displays intervals of mudrocks and shales at the base and sandy layers at the top. In the Western region, the San Carlos Quarry section (C) displays intercalation of mudrocks and limestones of the Cansona Fm. The Western Cordillera section (D) shows folded beds of limestones, siliceous limestones, and mudrocks of the Nutibara Mb. Of the Penderisco Fm. In the Uramita-Dabeiba area. The Gorgonilla Island section (E) exhibits tuffaceous sandstones interbedded with mudrocks. The core in ANH-LA LOMA-1 section has depth numbers indicated.

Cesar-Rancheria Basin, consists in ~626-m-thick deposits of the Molino and Barco formations (Ucaldas-Minciencias-ANH, 2020). In the lower to middle part of the core (~626–~265 m), marine deposits of the Molino Formation comprise an interlayering of massive and laminated mudrocks, claystones, limestones (*mudstones*, *wackestones*, and *packstones*), and shales with bivalves, brachiopods, gastropods, and echinoderms fossils, which were interpreted as outer shelf deposits (Ucaldas-Minciencias-ANH, 2020). The Molino Formation is also found in the middle to upper part of the core (~266–~117 m), composed of very fine-to medium-grained, locally conglomeratic sandstones, which occasionally show horizontal lamination and heterolytic beds with wavy and lenticular lamination. These deposits are associated with external shelf-offshore and coastal plain deposits (Ucaldas-Minciencias-ANH, 2020). In the upper part of the core, above the Molino Formation, lie ~117 m of Barco Formation deposits (Figs. 2 and 3). They are characterized by interlayering of mudrocks and sandstones forming wavy and flaser lamination. Root traces and carbonized-woody fragments are abundant, and massive coal levels interbedded with carbonaceous massive and laminated mudrocks are locally recorded. This interval is characterized by lack of marine microfossils, abundant pollen and

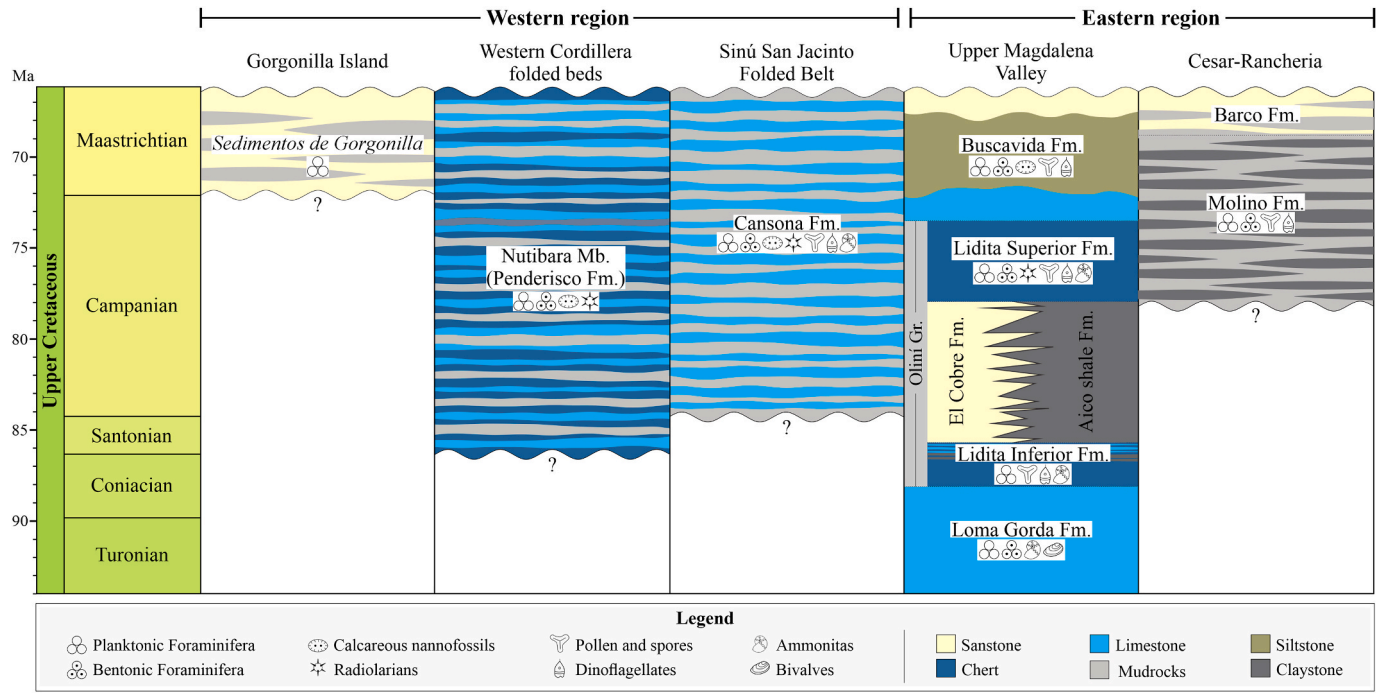

Fig. 3. Summary of available chronostratigraphic and lithostratigraphic information about the studied deposits. See text and Appendix A for further details.

spores, and scores of dinoflagellates. This segment has been interpreted as deltaic deposits (Ucaldas-Minciencias-ANH, 2020).

3.2. Western region

In the western region, we extracted calcareous nannofossils from moderately deformed deposits outcropping in the SSJFB and Isla Gorgonilla in the Tumaco Offshore Basin, as well as from highly deformed and segmented rocks of the Western Cordillera (Fig. 2C–E and 3). The stratigraphic section of the San Carlos Quarry in the SSJFB is composed of ~20 m of medium to thin bioturbated tabular strata of laminated mudrocks interbedded with massive limestones (*mudstones*); occasionally these strata are interlayered with siliceous mudrocks (Fig. 2C). These rocks, belonging to the Cansona Formation (Fig. 2C), are some of the oldest sedimentary deposits documented in the SSJFB (Duque-Caro, 1972a,b; Geotec, 2003). The analyzed samples from the highly deformed deposits from the Western Cordillera were collected from the best exposures along the Uramita-Dabeiba, El Sireno, and Santa Cecilia roads (Fig. 2D). These strongly folded and faulted outcrops are composed of an alternation of thin tabular strata of limestones and cherts, which are interlayered with greenish bioturbated mudrocks. These rocks belong to the Nutibara Member of the Penderisco Formation (Álvarez and Gonzáles, 1978). Owing to sedimentological and ichnological features, these rocks, together with those of the Cansona Formation, are interpreted as pelagic and hemipelagic deposits accumulated in deep marine environments (Pardo-Trujillo et al., 2020; Giraldo-Villegas et al., 2023). The Gorgonilla section consists of an alternation of laminated mudrocks and sandstones (locally conglomeratic) bearing fossils of radiolaria, benthic foraminifera, mollusks, and corals (Fig. 2E). Bermúdez et al. (2016, 2019) described these deposits as an intercalation of tuffaceous sandstones, marls, siltstones, and massive gray-yellow tuffaceous clays with soft-sedimentary deformation structures and tektites, which represent turbidites accumulated in bathyal and pelagic environments. These rocks are informally known as *Sedimentos de Gorgonilla* (Bermúdez et al., 2019).

4. Previous biostratigraphic studies

The age assigned to the studied deposits has been mainly based on macrofossils and microfossils such as ammonites, bivalves, foraminifera, palynomorphs, and calcareous nannofossils (Fig. 3 and Appendix A). According to our review, biostratigraphic information for marine deposits from the eastern region is more extensive than for rocks from the western region, which can be explained by higher oil exploration activity in the Magdalena Valley and Cesar-Rancheria basins (Fig. 3). In the eastern region, chronostratigraphy of marine deposits, initially based on well-preserved ammonites and bivalves, displayed an age range from Turonian to Santonian (Bürgl and Dumit, 1954; Bürgl, 1961; Etayo et al., 1969; Etayo-Serna, 1979; Patarroyo, 2011; Patarroyo and Bengtson, 2017; Patarroyo et al., 2017). This biostratigraphic framework was reinforced by data derived from palynomorphs (Solé de Porta, 1972; Jaramillo and Yepes, 1994), micropaleontology, foraminifera (Bürgl and Dumit, 1954; Petters, 1955; Vergara, 1994, 1997; Guerrero et al., 2000; Martínez, 2003; Navarrete-Parra et al., 2018) and calcareous nannofossils (De Romero et al., 2003; Pérez et al., 2018; Páez-Reyes et al., 2021). These studies, showing well-preserved foraminifera and palynomorphs (Bürgl and Dumit, 1954; Gandolfi, 1955; Petters, 1955; Bürgl, 1961; Martínez, 1989, 2003; Dueñas, 1989; Martínez and Hernandez, 1992; Jaramillo and Yepes, 1994; Vergara, 1997; Guerrero et al., 2000; Tchegliakova and Mojica, 2001; Yepes, 2001; Terraza-Melo et al., 2002) and scarce calcareous nannofossils (Tchegliakova and Mojica, 2001), particularly helped to improve age constraints for Campanian–Maastrichtian marine deposits. Among these earlier studies, Martínez (2003), Jaramillo and Yepes (1994), and Garzon et al. (2012) built some of the most complete foraminiferal and palynological biozonations for Turonian–Maastrichtian deposits for the UMV. Similarly, the pioneering study of Pérez et al. (2018) contributed to Coniacian–Campanian calcareous nannofossil biostratigraphy of deposits of the La Luna Formation in the Middle Magdalena Valley (MMV). Finally, the studies of Martínez (1989) and Yepes (2001), based on foraminifera and palynomorphs, respectively, provided useful biostratigraphic information for Campanian–Maastrichtian deposits in the Cesar-Rancheria Basin (Fig. 3).

The available biostratigraphic information for Upper Cretaceous

marine deposits from the western region indicates an age range from Coniacian to Maastrichtian (Fig. 3 and Appendix A). Published data show that age control of the Coniacian–Maastrichtian marine deposits from the SSJFB relied mainly on foraminifera (Chenevart, 1963; Duque-Caro, 1967a, 1967b, 1972a, 1967b; Geotec, 1997, 2003; Clavijo and Barrera, 2001; Guzmán, 2007; Herrera et al., 2009; Barrantes et al., 2019), although there are a few studies based on palynological results conducted by Dueñas and Gómez (2013). The age of sedimentation of these deposits has also been addressed by studies on ammonites and bivalves (Etayo-Serna et al., 1982; Duque-Caro, 1972a, 1972b, 1973); however, their biostratigraphic value has been questioned because of the abundant reworked fossils in these deposits (Duque-Caro, 1967b, 1972a, b; Etayo-Serna, 1989). Biostratigraphic studies from the Gorgonilla Island, based mostly on foraminiferal assemblages, suggest an age near the Cretaceous/Paleogene boundary (Bermúdez et al., 2016; Renne et al., 2018; Bermúdez et al., 2019). Age determinations for marine deposits from the Western Cordillera are based on ammonites, bivalves (Etayo-Serna, 1985, 1989; Moreno-Sánchez et al., 2002; Gómez-Cruz et al., 2002; Pardo-Trujillo et al., 2002a, b; Rodríguez and Arango, 2013; Díaz-Cañas and Patarroyo, 2014), and some mentions of foraminiferal and calcareous nannofossil assemblages, which are described as poorly preserved and rarely abundant (Barrero, 1979; Théry, 1980; Etayo--Serna et al., 1982; 1990; Pardo-Trujillo et al., 2002b; Patiño et al., 2019; Pardo-Trujillo et al., 2020). These previous studies indicate age ranges of Coniacian? To Maastrichtian (Fig. 3).

5. Methodology

We analyzed calcareous nannofossils from 119 rock samples distributed over nine localities (Fig. 1A; Table 1). Analyzed samples from the eastern area were collected from two stratigraphic sections, one cropping out along the Aico Creek section in the UMV and one cored-section named the ANH-LA LOMA-1 and drilled by the *Agencia Nacional de Hidrocarburos* (ANH) in the Cesar-Rancheria Basin (Fig. 1A). The samples from the western region belong to two stratigraphic sections, one outcropping in the San Carlos Quarry in the SSJFB of the Caribbean region and one from the Gorgonilla Island in the Tumaco Offshore in the Pacific region (Fig. 1A). In addition to this, we sampled five localities of folded-bed outcrops from the Western Cordillera (Table 1). Sampling resolution varies depending on the thickness and state of preservation of the outcrops. Samples were taken every meter in the San Carlos Quarry (~20 m thick) and every one to 2 m in the Gorgonilla Island (~11 m thick), whereas samples from the Western Cordillera lack consecutive sampling because of discontinuity and extensive deformation of the outcrops (Table 1). In the Aico Creek section (~284 m thick), sampling was performed every ~15 m, and in the ANH-LA LOMA-1 core (~626 m in thickness), every ~10 m. We used the classification of for siliciclastic rocks with grain size <63 μm and for limestones.

Slides of calcareous nannofossils were prepared using the standard technique of the smear slide (Bown and Young, 1998). Quantitative analyses of nannofossils were done using a Nikon polarized light microscope at 1000× magnification and counting up to ~600 fields of view (Appendix B). We used the qualitative scale of Roth and Thierstein (1972) to evaluate preservation of calcareous nannofossils: (G) good preservation: scarce or no evidence of dissolution and/or recrystallization, (M) moderate preservation: slightly dissolved and/or recrystallized microfossils, and (P) poor preservation: species strongly dissolved and/or recrystallized microfossils. Determination of calcareous nannofossils relied on taxonomic schemes of Bown and Young (1997) and Perch-Nielsen (1985), as well as information available on the online database Nannotax Our biostratigraphic analysis was based on the Upper Cretaceous standard biozonations for low-latitude by Sissingh (1977, 1978) and Burnett (1998). We used the chronostratigraphic framework and nomenclature of the International Subcommission on Cretaceous Stratigraphy https://stratigraphy.org/.

6. Calcareous nannofossil assemblages and biostratigraphic assignments

Micropaleontological analyses show 35 (morpho) genera and 50 (morpho) species of calcareous nannofossils (Fig. 4, Appendix B). Nannofossils from the eastern deposits were rarely to commonly abundant and assemblages were dominated by *Watznaueria* and *Micula*. This assemblage was accompanied by *Prediscosphaera*, *Cribrosphaerella*, and *Retecapsa*, in the Aico Creek section and peaks of abundance of *Kamptnerius magnificus* in the ANH-LA LOMA-1 core (Fig. 4, Appendix B). Nannofossil abundance from the western stratigraphic sections ranged from common to very abundant, and calcareous nannofossils were dominated by the genera of *Watznaueria*, *Micula*, and *Uniplanarius* (Fig. 4, Appendix B). Preservation of microfossils varied from poorly to well preserved in eastern deposits, but preservation was uniformly poor in western deposits (Appendix B). We observed that eastern deposits yield a higher variety of taxa (73%) in comparison to nannofossils recovered from western rocks (27%). In contrast, our counts show that western samples have higher abundance of calcareous nannofossils (54%) than eastern samples (46%) (Appendix B). Among the studied sections from the eastern region, micropaleontological assemblages of the ANH-LA LOMA-1 core were more diverse but less abundant than those from the Aico Creek. The analyzed sections of the San Carlos Quarry and El Purgatorio Quarry, together with the Gorgonilla Island, recorded the most abundant and diverse nannofossils among the western sections (Appendix B).

6.1. Aico Creek section

Micropaleontological results from the Aico Creek section showed that calcareous nannofossils are poorly to moderately preserved and abundance can vary from rare to very abundant. A total of 20 genera were quantified in this section. The most abundant genera were *Watznaueria* (63%) and *Micula* (19%); taxa of lower abundance were

Table 1
Studied localities with their respective lithostratigraphic information, number of analyzed samples, thickness and/or depth. Three types of deposits were sampled: slightly deformed outcrops (O: outcrops), cored-stratigraphic section (C: core), and highly folded outcrops (CP: check point).

Region	Locality	Location	Lithostratigraphic unit	Coordinates		Number of samples	O/C/CP
Eastern region	1	ANH-LA LOMA-1 cored-stratigraphic section	Molino Fm.	9°37′56.26″N	73°28′36,01″W	58	C (~626 m)
	2	Aico Creek	Loma Gorda, Buscavida fms. and Oliní Group	3°42′49.62″N	75°31′25.13″O	20	O (~284 m)
Western region	3	San Carlos Quarry	Cansona Fm.	9°14′38.28″N	75°47′18.07″W	21	O (~20 m)
	4	Gorgonilla Island	*Sedimentos de Gorgonilla*	2°56′00″N	78°12′00″W	8	O (~11 m)
	5	El Purgatorio Quarry	Cansona Fm.	8°41′11.26″N	75°50′0.85″W	1	CP
	6	Road Uramita-Dabeiba	Nutibara Mb. (Penderisco Fm.)	6°54′47.38″N	76°13′19.97″W	6	CP
	7	El Sireno Pathway	Nutibara Mb. (Penderisco Fm.)	6°23′20.42″N	76°14′51.99″W	1	CP
	8	Road to Santa Cecilia	Nutibara Mb. (Penderisco Fm.)	5°20′51.50″N	76° 6′28.33″W	1	CP
	9	El Naranjo Quarry	Cisneros Fm.	3°46′56.14″N	76°43′12.88″W	3	CP

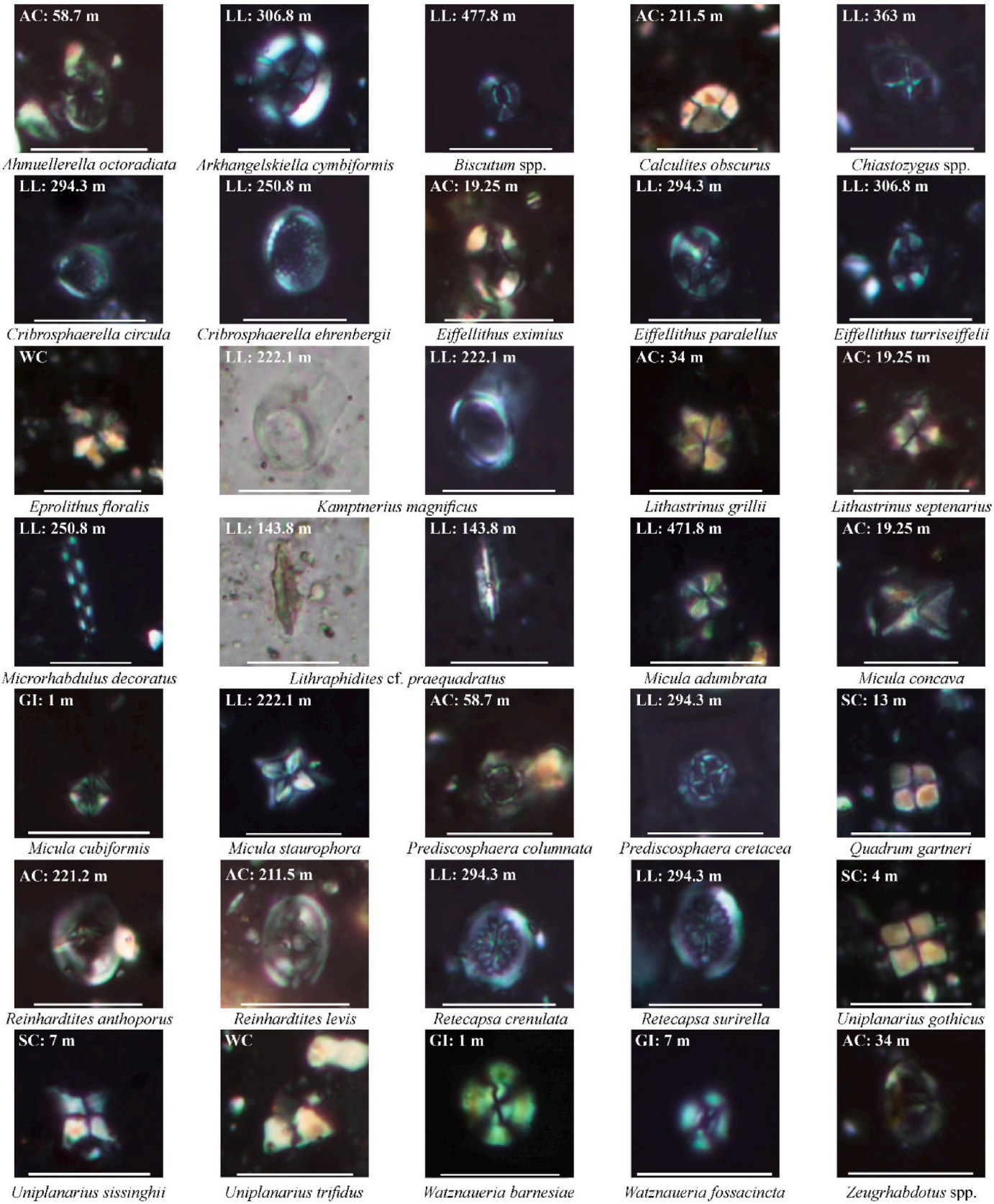

Fig. 4. Microphotographs of key calcareous nannofossil taxa identified in this work. (AC): Aico Creek section. (LL): ANH-LA LOMA-1 cored-stratigraphic section, (WC)*: Western Cordillera, (SC): San Carlos Quarry section, (GI): Gorgonilla Island section. Scale bar = 10 μm *Calcareous nannofossils from folded beds.

Prediscosphaera (4%), *Retecapsa* (3%), *Cribrosphaerella* (2%), *Zeugrhabdotus* (2%), *Eiffellithus* (1%), *Uniplanarius* (1%), and *Reinhardtites* (1%) (Appendix B). In the base of the section (from ~7 m to ~13 m), calcareous nannofossils were rare and their preservation was poor; we recovered only sporadic forms of *Quadrum gartneri* from ~9 m. This biozonal marker, whose first appearance occurs at the beginning of zone UC7 (CC11), indicates an age not older than early Turonian (Fig. 5). The abundance and preservation of nannofossils improved after ~19 m, when the biozonal marker *Micula concava* appeared for the first time. This taxon has its first appearance in zone UC11c (CC16) of the upper Coniacian (Burnett, 1998; Sissingh, 1977), thus constraining the interval between ~9 m and ~19 m (~10 m thick) to a zonal range from UC7 to UC11b (CC11 to CC15), equivalent to an age range from lower Turonian to Coniacian (Fig. 5). The UC11c (CC16) biozone is delimited by the first occurrence of *M. concava* and the last occurrence of *Lithastrinus septenarius* (Burnett, 1998). Although these bioevents were not identified in the section, both taxa were recovered simultaneously at ~34 m, corroborating the presence of this biozone and assigning an age range from upper Coniacian to lower Santonian to this part of the section. The biozonal marker *Lithastrinus grillii*, which appears for the first time in the base of zone UC11, was similarly found at ~34 m, supporting our zonal assignment of UC11c (Fig. 5). Above this interval, nannofossil counts revealed the first occurrence of *A. cymbiformis* at ~59 m and the absence of *L. septenarius* and *L. grillii*, which became extinct for the rest of the section. The first occurrence of *A. cymbiformis* defines the base of the zone UC13 of Burnett (1998), equivalent to CC17 biozone of Sissingh (1977), close to the Santonian/Campanian boundary. Therefore, the stratigraphic interval between ~34 m and ~59 m (~24.7 m) is restricted to zone UC12 (Burnett, 1998) and biozonal range CC16-17 (Sissingh, 1977), thus indicating an age range from Santonian to the lower Campanian (Fig. 5). Micropaleontological recovery from ~59 m up to ~156 m (~97 m) was characterized by two samples that contain poorly preserved taxa of *Eiffellithus* spp., *Micula* spp., *Prediscosphaera* spp., *Retecapsa* spp., and *Watznaueria* spp., making biostratigraphic constraints difficult in this part of the section. However, the first occurrence of *Uniplanarius trifidus* at ~156 m indicates that this level cannot be older than zone UC15d of the upper Campanian and helps to restrict the interval between ~59 and ~156 m to biozones UC13–UC15c (CC17–CC21), equivalent to the lower part of Campanian (Fig. 5). An increase in preservation and abundance after ~221 m enabled us to observe the co-occurrence of *Reinhardtites anthophorus* and *U. trifidus*, confirming that the interval between ~156 m and ~221 m (~65 m) belongs to the UC15d–UC15e (CC22) subzones of the upper Campanian (Fig. 5). Subsequently, calcareous nannofossils showed a decline in preservation and abundance from ~237 m until the extinction of several taxa at ~259 m (Fig. 5). Among them, *U. trifidus* and *Reinhardtites levis* were observed for the last time at this level, denoting the top of biozones UC17 (CC23b) and UC18 (CC24), respectively, of the early Maastrichtian. These biostratigraphic markers help to constrain the upper part of the section to biozones UC16–UC17 (Burnett, 1998) and CC23 (Sissingh, 1977), indicating an age range from the uppermost Campanian to lowermost Maastrichtian (Fig. 5). This age is also supported by the common occurrence at ~259.5 m of *Uniplanarius sissinghii*, which has its last occurrence in the early Maastrichtian (Burnett, 1998). In the last analyzed sample at, ~282 m, calcareous nannofossils were poorly preserved and scarce, having an assemblage composed of *Micula* spp., *Retecapsa* spp., and *Watznaueria* spp. (Appendix B). These genera are characterized by their wide biostratigraphic range during the Late Cretaceous, making it difficult to establish the age more precisely. Although the number of identified reworked taxa in the section was low, some specimens of *P. columnata* occur sporadically between ~19 m and ~221 m. This taxon, which has a biostratigraphic distribution from the Albian to Turonian (Burnett, 1998), was found together with younger assemblages from the Coniacian to Maastrichtian (Fig. 5). In summary, the Aico Creek section between ~9 m and ~259 m covers a biozonal range from undifferentiated zones UC7–UC11b (CC11) to UC16–?UC17 (?CC23), which is equivalent to an age range from Turonian–Coniacian to the latest Campanian–early Maastrichtian (Fig. 5).

6.2. ANH-LA LOMA-1 cored-stratigraphic section

Micropaleontological analyses from this cored-stratigraphic section show that 26 samples were barren and 32 yielded calcareous nannofossils with moderate to good preservation and few to common in abundance (Fig. 6; Appendix B). The recovered assemblages were diverse (29 genera) but dominated by high abundance of *Micula* (29%), *Watznaueria* (20%), and *K. magnificus* (19%), followed by *Prediscosphaera* (4%), *Chiastozygus* (4%), *Cribrosphaerella* (3%), *Retecapsa* (3%), *Zeugrhabdotus* (3%), *Eiffellithus* (37%), *Microrhabdulus* (2%), *Calculites* (2%) and *Staurolithites* (1%) (Appendix B). Examined samples from the basal part of the core (first ~21 m) are barren, but several peaks of poorly and well-preserved nannofossils occurred between ~599 m and ~144 m (Fig. 6). Abundance and preservation of microfossils improved from ~204 m to ~313 m before they dramatically disappeared after ~138 m in the upper part of the core (Fig. 6). From ~599 m to ~144 m we identified the sporadic occurrence of *Arkhangelskiella cymbiformis, Calculites obscurus*, *Micula staurophora*, and *Prediscosphaera cretacea,* indicating a zonal range from UC13 (UC13a in boreal provinces) to UC20 (CC17–CC26) of the early Campanian to Maastrichtian interval (Fig. 6). This biozonal assignment is supported by the recovery of *Lithraphidites* cf. *praequadratus* at ~144 m, which is a biostratigraphic marker commonly used for recognition of zones UC15d–UC20 (CC22–CC26) of the Campanian–Maastrichtian (Roth, 1978; Burnett, 1998). Quantitative results also show that *Micula adumbrata*, which has a biostratigraphic range from Turonian to Coniacian (Sissingh, 1977; Burnett, 1998), was found irregularly between ~144 m and ~295 m, indicating reworking of older Upper Cretaceous deposits. Likewise, the recovery at ~313 m of *Prediscosphaera columnata*, whose last occurrence has been registered in the Turonian (Burnett, 1998), also indicates the presence of reworking in this core (Appendix B).

6.3. San Carlos Quarry section

Our analyses showed abundance patterns that vary from common to very abundant in the first ~13 m of the section and from few to barren from ~14 m up to the top (Fig. 7). Nannofossils were generally poorly preserved, showing overgrowth and recrystallization; however, moderate preservation of some taxa allowed taxonomic determination (Figs. 7 and 4). Our counts indicate the recovery of an assemblage dominated by high abundance of *Watznaueria* (61%), *Micula* (23%), and *Uniplanarius* (11%) and containing low occurrences of *Quadrum* (3%) and *Retecapsa* (2%) (Appendix B). Our counts revealed a uniform assemblage characterized by the co-occurrences of *U. sissinghii* and *U. trifidus*, whose appearance denotes the base of UC15d biozone, suggesting that the basal segment of the section cannot be older than zone UC15d (CC22) of the upper Campanian (Burnett, 1998; Sissingh, 1977) (Fig. 7). Likewise, the continuous record of *U. trifidus* and *U. gothicus* up to ~13 m indicates that this stratigraphic level is not younger than UC17 (CC23), since these species have their last occurrence in the early Maastrichtian (Sissingh, 1977; Burnett, 1998). Therefore, the interval between 0 and ~13 m is restricted to the biozonal range UC15d–UC17 (CC22– CC23) of the upper Campanian–lower Maastrichtian. At ~14 m abundance of calcareous nannofossils changed markedly, with distribution patterns becoming discontinuous due to the absence of nannofossils in some samples up to the top of the section (Fig. 7). The observed assemblage in this interval (last ~6 m of the section) consisted of sporadic forms of *Micula* spp., *Watznaueria* spp., *Q. gartneri*, and *Retecapsa* spp. Although this association is characteristic of the Late Cretaceous, the scarce recovery prevented us from performing a more detailed biostratigraphic analysis.

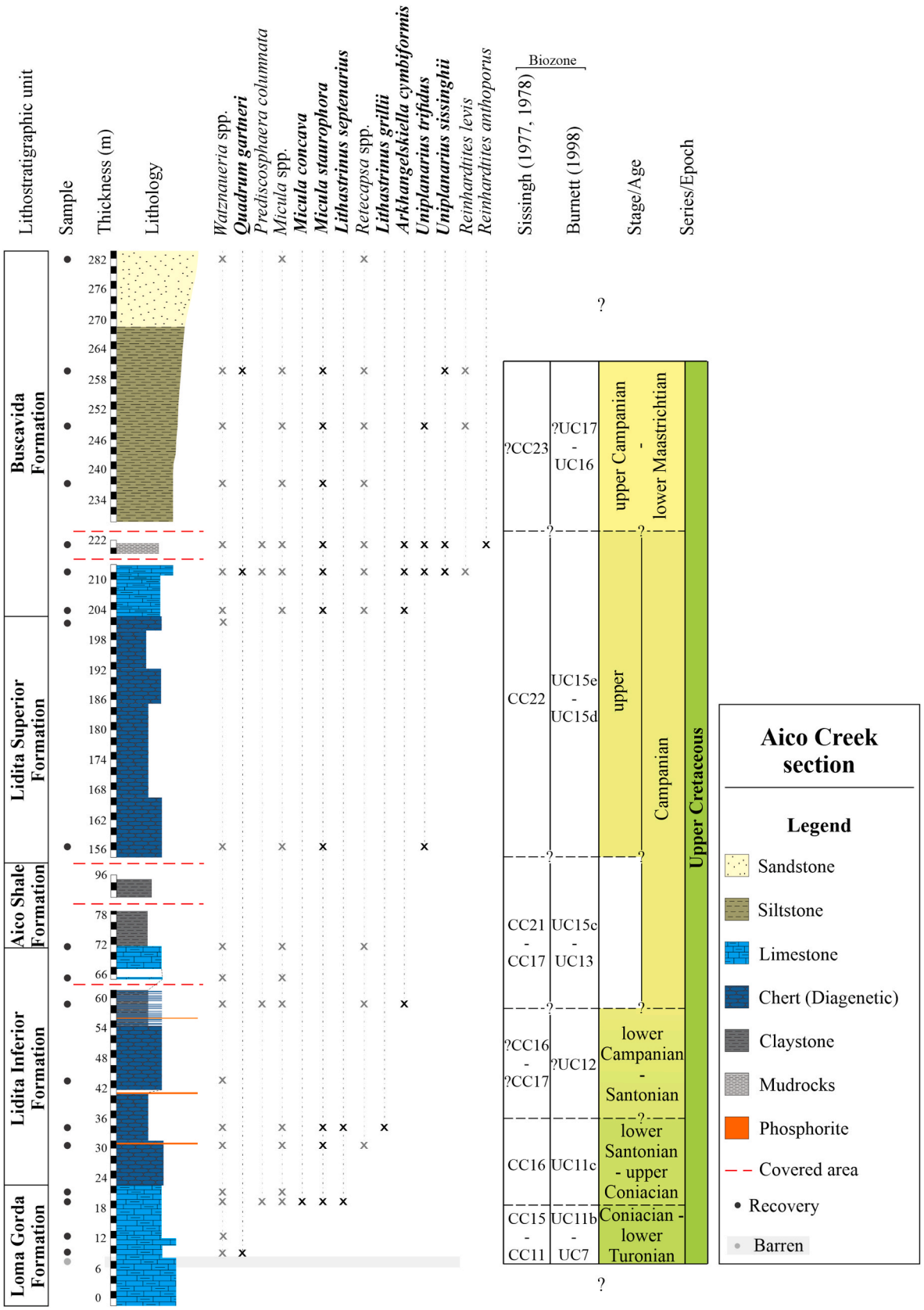

Fig. 5. Distribution patterns of the calcareous nannofossil markers (in bold), biozonal assignments, and age constraints of the Aico Creek section. "X" represents the presence of the specimen in the sample. The stratigraphic log was taken from Hernández (2021).

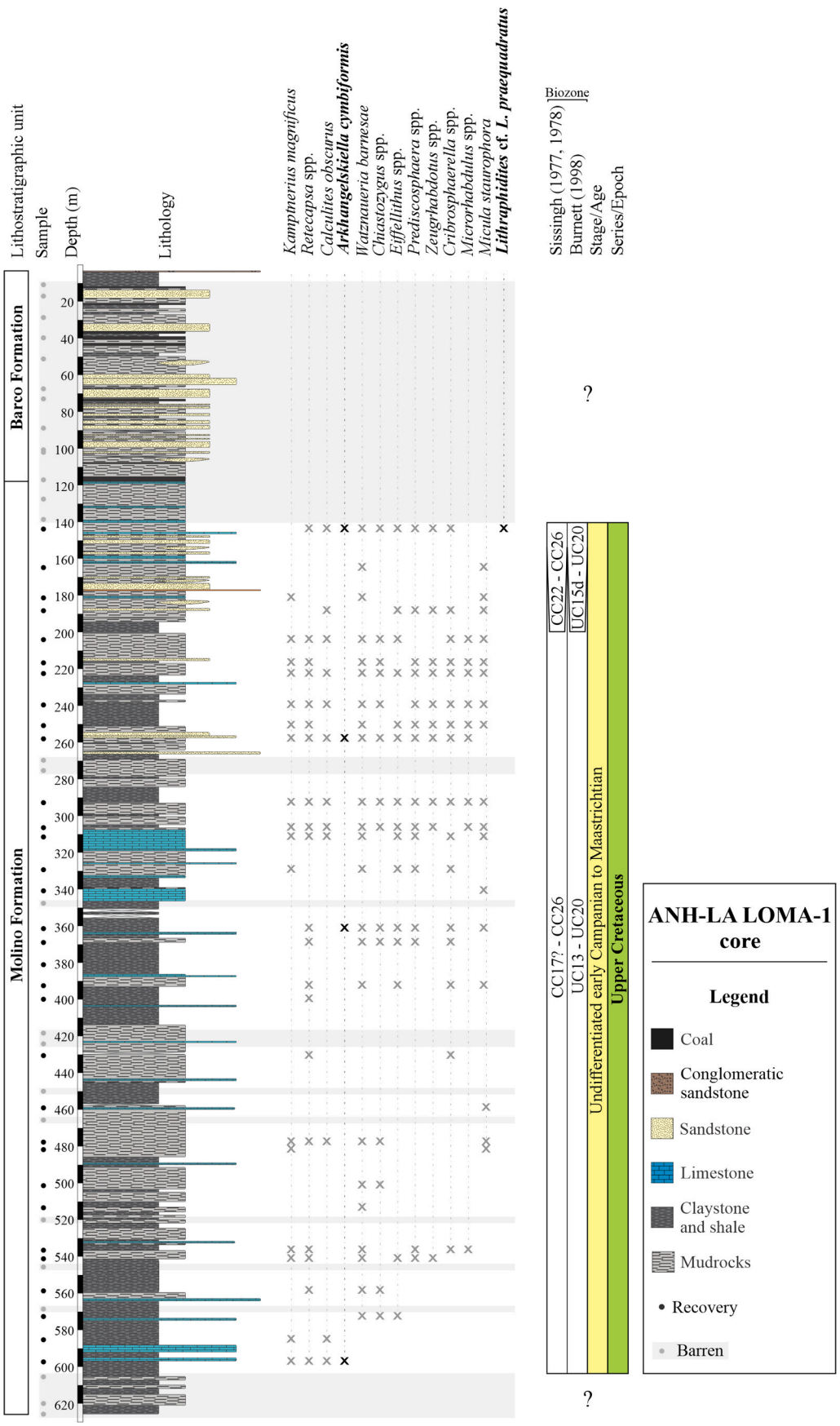

Fig. 6. Distribution patterns of the calcareous nannofossil markers (in bold), biozonal assignments, and age constraints of the ANH-LA LOMA-1 cored-stratigraphic section. "X" represents the presence of the specimen in the sample. Stratigraphic log taken from Ucaldas-Minciencias-ANH (2020).

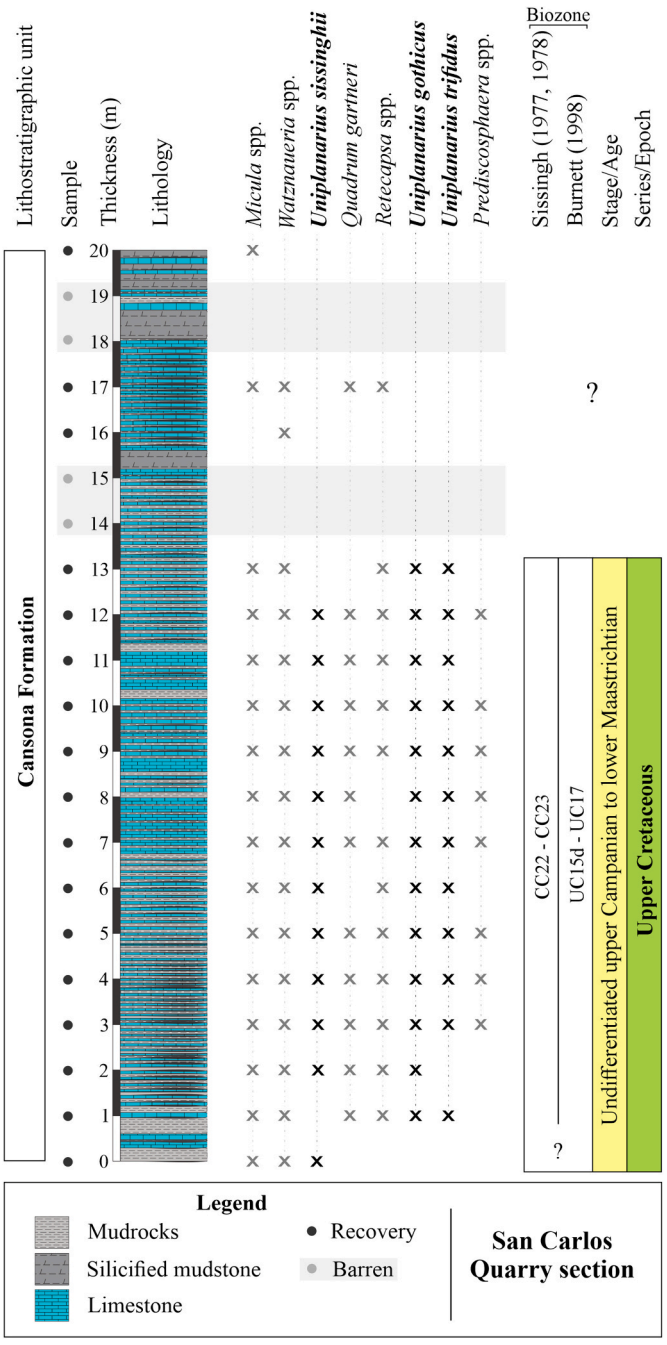

Fig. 7. Distribution patterns of the calcareous nannofossil markers (in bold), biozonal assignments, and age constraints of the San Carlos Quarry stratigraphic section. "X" represents the presence of the specimen in the sample. Stratigraphic log taken from Giraldo-Villegas et al., 2023.

6.4. Gorgonilla Island section

The biostratigraphic information of this section is based on eight samples (Fig. 8). Micropaleontological analyses revealed samples with rare to abundant recovery of nannofossils, and three samples that were barren (Fig. 8, Appendix B). Preservation of microfossils from these samples ranged from poor to moderate, with some recrystallized and occasionally dissolved specimens (Fig. 8). Micropaleontological assemblages were dominated by *Micula* spp. (57%) and *Watznaueria* spp. (32%) and characterized by a high diversity of forms such as *Arkhangelskiella cymbiformis, K. magnificus, Microrhabdulus* spp., *Retecapsa* spp., *Cribrosphaerella* spp., *U. trifidus*, *Calculites* spp., *Biscutum* spp., and

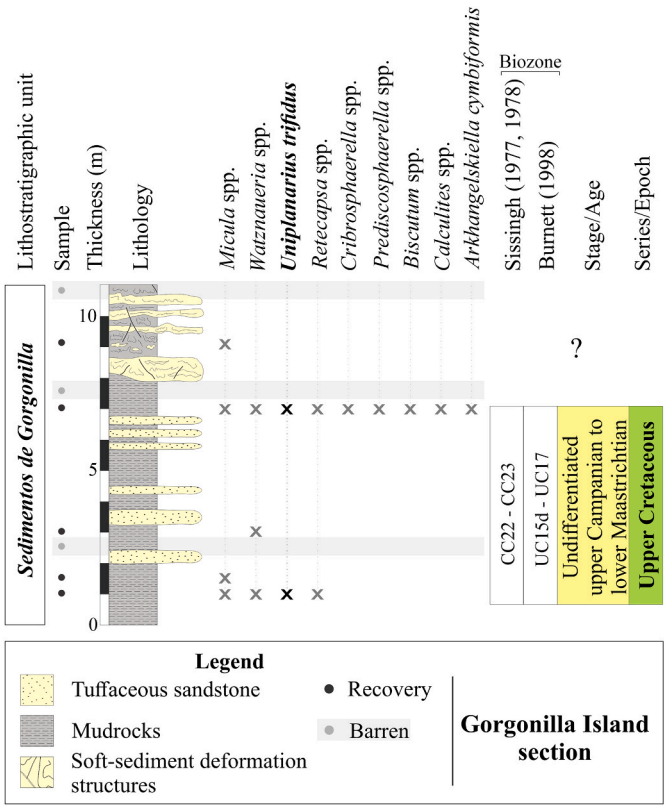

Fig. 8. Distribution patterns of the calcareous nannofossil markers (in bold), biozonal assignments, and age constraints of the Gorgonilla Island stratigraphic section. "X" represents the presence of the specimen in the sample. The stratigraphic log was taken from (Universidadde Caldas, 2012).

Prediscosphaera spp. The biozonal marker *U. trifidus* was observed sporadically at 1 and 7 m along with *A. cymbiformis* and *M. staurophora* (Fig. 8). The occurrence of these taxa frames this stratigraphic interval between zones UC15d and UC17 (CC22–CC23), corresponding to the upper Campanian–lower Maastrichtian interval (Fig. 8). Nannofossil analyses showed a decrease in abundance above ~7 m, including two barren samples. The assemblage identified between ~7 and ~11 m consisted of *Micula* spp. and *Watznaueria* spp., which are indicative of the Late Cretaceous. However, the poor recovery in this interval does not allow us to place further biostratigraphic constraints or rule out reworking (Fig. 8).

6.5. Folded outcrops of the Western Cordillera

Our micropaleontological analyses from the folded deposits of the Western Cordillera showed that samples from the El Naranjo Quarry and Santa Cecilia outcrops were barren; calcareous nannofossils were recovered from the El Purgatorio Quarry, Uramita-Dabeiba, and El Sireno outcrops (Fig. 9), but these were assemblages with poor preservation. The examined sample from the El Purgatorio Quarry showed abundant nannofossils of *Micula* (79%), and lesser abundance of *Watznaueria* (14%), *Retecapsa* (4%), *Uniplanarius* (3%), and *Quadrum* (1%) (Fig. 9A). Nannofossils recovered from samples of the El Sireno Pathway had similarly a predominance of *Watznaueria* (98%), which was accompanied by scarce abundance of *Uniplanarius* spp. (1.3%) and *Calculites obscurus* (0.4%) (Fig. 9B). The collected samples along the Uramita-Dabeiba road displayed rare to very abundant microfossils with abundant species of *Watznaueria* (88%) and sporadic forms of *Micula* spp. (9%), *Uniplanarius* spp. (3%), and *Quadrum gartneri* (0.2%) (Fig. 9C). Micropaleontological assemblages from these localities are characterized by the co-occurrence of the nannofossil markers *U. trifidus*

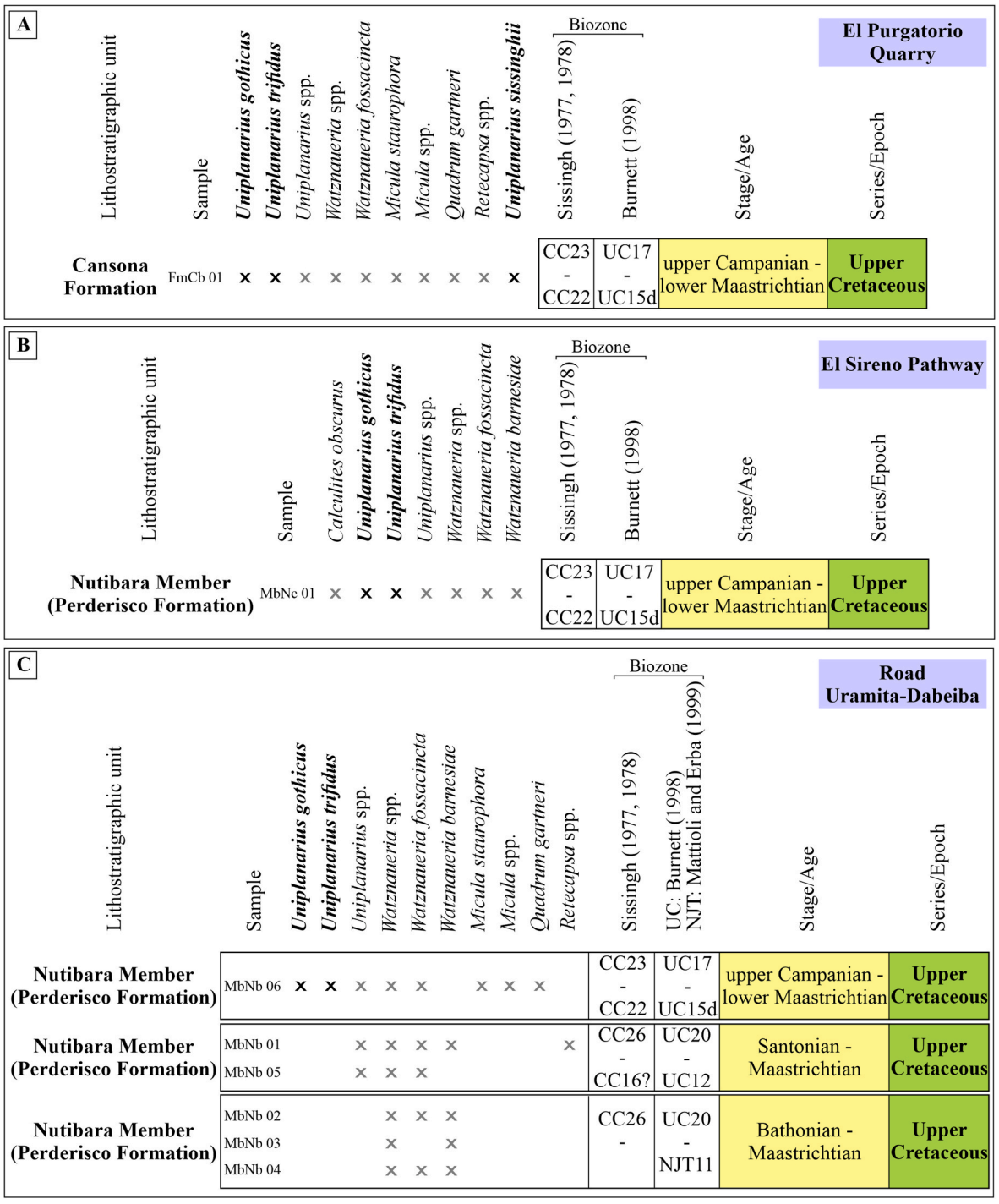

Fig. 9. Distribution patterns of the calcareous nannofossil markers (in bold), biozonal assignments, and age of taxa discovered in folded deposits of the Western Cordillera. "X" represents the presence of the specimen in the sample.

and *U. gothicus*. These taxa coexisted between biozones UC15d and UC17 (CC22 and CC23), indicating an age range from late Campanian to early Maastrichtian (Fig. 9). In the El Purgatorio Quarry, this age is corroborated by the presence of *U. sissinghi*, whose first appearance occurred in zone UC15c (CC21), indicating an age not older than late Campanian (Fig. 9). In addition, our biozonal and age ranges suggest that the presence of *Eprolithus floralis*, whose biostratigraphic interval is restricted to an Albian–early Campanian age (Burnett, 1998), is indicative of reworking in samples from the Uramita-Dabeiba road.

7. Discussion

7.1. Biostratigraphic comparison with previous studies from the Magdalena Valley basin

Micropaleontological analyses from the Aico Creek section in the UMV show calcareous nannofossil assemblages of Turonian–Maastrichtian age, covering the longest biostratigraphic interval among the studied sections (Figs. 5 and 9). This provides an opportunity to correlate our results with well-studied stratigraphic sections of the Upper Cretaceous in the Magdalena Valley Basin. According to previous

studies, the Loma Gorda Fm., which represents the base of the Aico Creek section (Hernández, 2021), was deposited from the Turonian to early Santonian (Bürgl and Dumit, 1954; Bürgl, 1961; Martínez, 2003; Patarroyo, 2011). This is consistent with the first occurrences of *Q. gartneri* at ~9 m and *M. concava* at ~19 m, thus restricting a part of the Loma Gorda Fm. In our section to nannofossil biozones UC7 (CC11)–UC11c (CC16) of the early Turonian–Coniacian (Fig. 5). Although our data preclude a more detailed biostratigraphic analysis for this interval, our interpretation correlates well with the biozone *Micula adumbrata*–Micula adumbrate–Micula concava of Pérez et al. (2018) for the base of the La Luna Fm. In the MMV Basin. Deposits of the Oliní Group (Lidita Inferior Fm.), which rests conformably over the Loma Gorda Fm., have been dated as Coniacian–Santonian (Bürgl and Dumit, 1954; Jaramillo and Yepes, 1994; Guerrero et al., 2000; Tchegliakova and Mojica, 2001; Garzon et al., 2012) (Appendix A). Furthermore, palynological data have suggested that the Coniacian/Santonian boundary can be placed on this formation in the Aico Creek section (Jaramillo and Yepes, 1994; Garzon et al., 2012). This agrees with the last occurrence of *L. septenarius* in the base of the Lidita Inferior Fm. (~34 m), marking the top of the biozone UC11c (CC16) and indicating an age range from late Coniacian to early Santonian (Fig. 5). A similar age range was proposed for the Micula concava biozone in the lower part of the La Luna Fm. (Pérez et al., 2018); however, their interpretation was based on *Eprolithus* spp., a taxon with rare abundance in the Aico Creek section. The first occurrence of *A. cymbiformis* (~59 m), which denotes the base of UC13 biozone (upper part of CC17) near the Santonian/Campanian boundary (Burnett, 1998; Dubicka et al., 2017; Kita et al., 2017; Wolfgring et al., 2018; Miniati et al., 2020), was found in upper deposits of the Lidita Inferior Fm. (Hernández, 2021). However, previous biostratigraphic information from the Aico Creek section and other localities in the Magdalena Valley revealed that this age is ascribed to sediments of the Aico Shale Fm. (stratigraphically equivalent to *Niveles de Lutitas*; El Cobre Fm.) (Jaramillo and Yepes, 1994; Tchegliakova and Mojica, 2001; Martínez, 2003; Garzon et al., 2012). Accordingly, we propose that the lithostratigraphic boundary between the Lidita Inferior and Aico Shale fms. proposed by Hernández (2021) be revised and, if necessary, positioned at lower stratigraphic levels in the Aico Creek section below the first occurrence of *A. cymbiformis* (Fig. 5). In the La Luna Fm. a stratigraphic gap has been described that covers the Santonian/Campanian boundary (Navarrete-Parra et al., 2018; Guerrero et al., 2021). However, our low sampling resolution prevents us from identifying this gap. The only bioevent identified in the base of the Lidita Superior Fm. was the first occurrence of *U. trifidus*, suggesting an upper Campanian age for these deposits (Fig. 10). This coincides with previous age assignments of the Lidita Superior Fm. as late Campanian to (Bürgl, 1961; Jaramillo and Yepes, 1994; Vergara, 1997; Guerrero et al., 2000; Tchegliakova and Mojica, 2001; Terraza-Melo et al., 2002; Martínez, 2003; Garzon et al., 2012) (Appendix A).

Calcareous nannofossil recovery improved in the base of the Buscavida Fm., including biostratigraphic markers *U. trifidus* and *U. sissinghii* and accompanying taxa *R. levis* and *R. anthophorus* (Figs. 5 and 9). The co-occurrence of *U. trifidus* and *U. sissinghii* indicates the biozonal range UC15d–UC17 (CC22–CC23), equivalent to the interval late Campanian–early Maastrichtian; the last occurrence of *R. anthophorus*, which marks the top of the UC15 biozone, denotes late Campanian (Burnett, 1998). This agrees with the late Campanian age previously proposed for the base of the Buscavida Fm. (Bürgl and Dumit, 1954; Petters, 1955; Vergara, 1997; Guerrero et al., 2000; Tchegliakova and Mojica, 2001; Terraza-Melo et al., 2002; Martínez, 2003; Garzon et al., 2012). However, the biostratigraphic value of the last occurrence of *R. anthophorus*

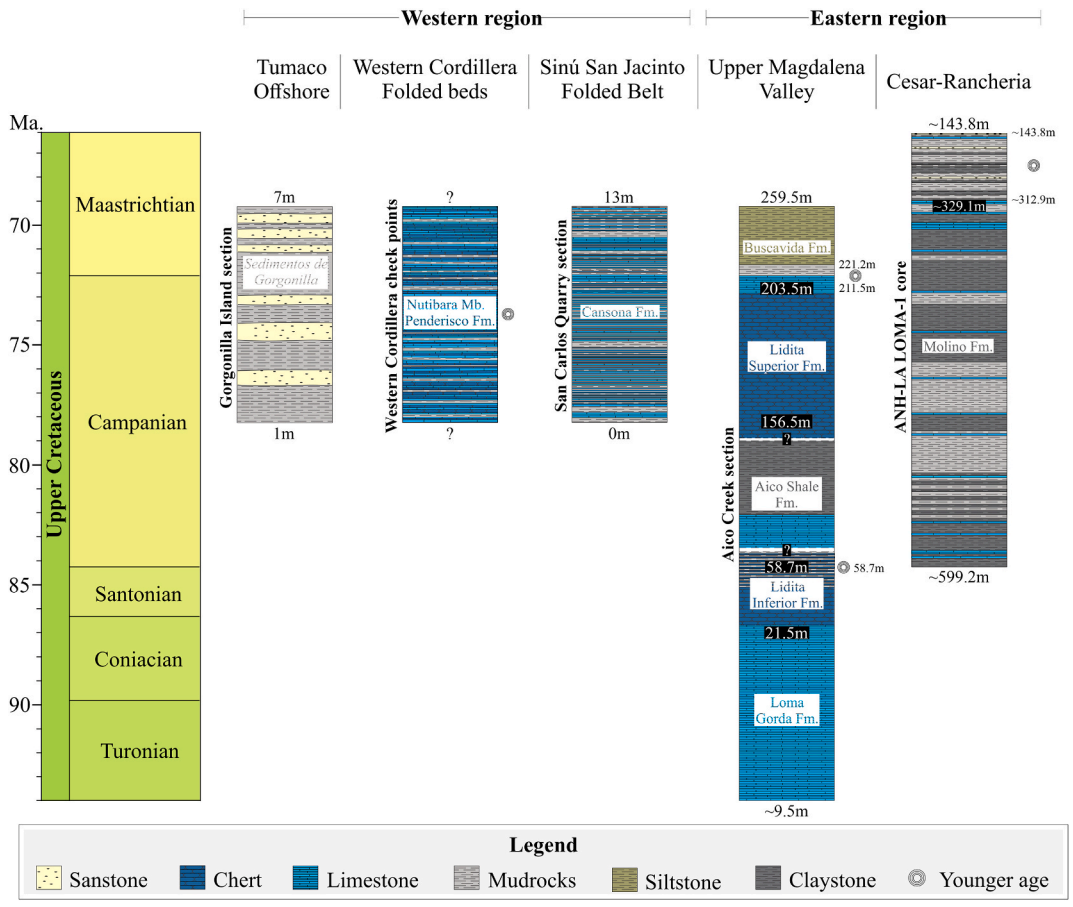

Fig. 10. Chronostratigraphic ranges indicated by calcareous nannofossil biostratigraphy for the studied deposits. These age ranges represent time intervals when sedimentation may have occurred, but calcareous nannofossil stratigraphy alone does not allow us to constrain this further or identify unconformities.

should be taken with caution because of documented reworking of this taxon in well-calibrated Maastrichtian sections (Burnett in Cunha et al., 1997; Jelby et al., 2014; Thibault et al., 2016). Instead, we recommend using the co-occurrence of *U. trifidus* and *U. sissinghii*, whose short biostratigraphic range makes them more reliable for determining the biozonal range UC15d–UC17 (CC22–CC23) of the late Campanian–early Maastrichtian (Fig. 5). In northern deposits of the Magdalena Valley Pérez et al. (2018) described a similar late Campanian age for the Umir Formation based on calcareous nannofossils *Eiffellithus parallelus* and *Broinsonia parca expansa*. However, these taxa did not appear in our analyzed samples.

7.2. Calcareous nannofossils biostratigraphy from the Cesar-Rancheria Basin

Previous biostratigraphic studies have dated the Upper Cretaceous deposits drilled by the ANH-LA LOMA-1 cored section as Maastrichtian and Campanian–Maastrichtian (Gandolfi, 1955; Petters, 1955; Dueñas, 1989; Martínez, 1989; Martínez and Hernández, 1992; Yepes, 2001; Patarroyo et al., 2022). These age ranges coincide with the occurrence of *A. cymbiformis*, which suggests a biozonal range from UC13 to UC20 (CC17 to CC26), extending from the early Campanian to Maastrichtian (Fig. 6). Nevertheless, additional low-latitude biostratigraphic markers were not observed in the studied samples even though the calcareous nannofossils from this locality were exceptionally well preserved, thus affecting biostratigraphic correlation with other Campanian–Maastrichtian assemblages (Fig. 6). The high abundances (or acmes) of *K. magnificus* (up to 19%) have been linked to cooler waters (Thierstein, 1981; Thibault and Gardin, 2006, 2007; Sheldon et al., 2010; Thibault et al., 2015a, b; Guerra et al., 2016). This is interpreted as evidence of changes in oceanic water conditions, which could have affected productivity and preservation of the low-latitude calcareous nannofossil markers and may possibly explain the low recovery of low-latitude taxa in our record. Furthermore, previous studies conducted on deep-sea sections near our studied area reported an increased in abundance of *K. magnificus* during the late Maastrichtian (Thibault and Gardin, 2006; Thibault et al., 2015a; Patarroyo et al., 2022). This could be correlated with the high abundance of *K. magnificus* found in our section between ~203.8 m and ~394.7 m, suggesting an upper Maastrichtian age for the upper part of the Molino Fm. In the deposits drilled by the ANH-LA LOMA-1 core (Fig. 10). This interpretation of cooling episodes is consistent with regional changes in oceanic water temperature in the proto-Caribbean Sea (Barrera and Savin, 1999; Linnert et al., 2014; O'Brien et al., 2017) and marine paleoproductivity in the La Luna Sea (Yepes, 2001; Martínez, 2003) during the Campanian and Maastrichtian.

7.3. Biostratigraphic correlation between eastern and western regions based on calcareous nannofossils

Analyzed samples from the San Carlos Quarry section in the SSJFB and the base of the Gorgonilla Island section, as well as highly folded deposits from the Western Cordillera, show a consistent recovery of *U. trifidus* and a sporadic occurrence of *U. sissinghii* and *U. gothicus* (Figs. 6–8). This suggests an accumulation age restricted to biozones UC15d (CC22)–UC17 (CC23) of the late Campanian–early Maastrichtian interval for the folded deposits of the western region (Fig. 10), which agrees with the Santonian to Maastrichtian age reported for the Nutibara Member (Penderisco Formation) in the Western Cordillera (Etayo-Serna et al., 1982; 1990; Patiño et al., 2019; Pardo-Trujillo et al., 2020) (Appendix A) and Campanian–Maastrichtian age for deposits of the Cansona Formation in the SSJB (Chenevart, 1963; Duque-Caro, 1967a,b, 1972a, b; Guzmán et al., 1994, 2004; Geotec, 1997, 2003; Clavijo and Barrera, 2001; Guzmán, 2007; Herrera et al., 2009; Dueñas and Gómez, 2013, Barrantes et al., 2019). Finally, the Campania–Maastrichtian age determined from calcareous nannofossil analyses is also in accordance with the Maastrichtian age based on foraminiferal analyses in the base of the Gorgonilla Island section in the Tumaco Offshore (Bermúdez et al., 2016; Renne et al., 2018; Bermúdez et al., 2019).

We notice that the assemblage *U. trifidus*, *U. sissinghii*, and *U. gothicus* was likewise observed in collected samples from the Lidita Superior and Buscavida formations of the Aico Creek section in the eastern region. As a result, upper Campanian–lower Maastrichtian deposits from both regions can be correlated, revealing that whereas western oceanic deposits of the Pacific and Caribbean basins accumulated over a Caribbean Plate oceanic basement close to the collision zone, eastern deposits were recording the vanishing of the La Luna Sea in the UMV (Villagómez et al., 2011; Villagómez and Spikings, 2013; Haq, 2014; Bayona, 2018; Pardo-Trujillo et al., 2020) (Fig. 10). These calcareous nannofossil assemblages, which are characterized by their low-latitude affinity (Thierstein, 1981; Burnett, 1998; Voigt et al., 2012), also support previous interpretations based on dinoflagellates, suggesting that a tropical oceanic connection between the allochthonous Caribbean Plate and the South American Plate occurred during the Campanian–Maastrichtian (Etayo et al., 1969; Fabre, 1985; Diaz, 1994; Martínez, 2003; Dueñas and Gómez, 2013).

8. Conclusions

The Upper Cretaceous deposits studied in the western and eastern basins of Colombia contain poorly to moderately preserved calcareous nannofossil assemblages, except for the well-preserved microfossils found in the Cesar-Rancheria Basin. Our biostratigraphic analysis shows that the Aico Creek section in the UMV was deposited between biozones UC7–UC11b (CC11) and UC16–?UC17 (?CC23), corresponding to an age range from the early Turonian–Coniacian to the late Campanian–Maastrichtian. Similarly, the ANH-LA LOMA-1 core from the Cesar-Rancheria Basin covers biozones UC13 to UC20 (CC17–CC26) and was deposited during the early Campanian–late Maastrichtian. Our dataset further reveals that the folded and faulted deposits of the SSJFB, Western Cordillera, and Gorgonilla Island section in Caribbean and Pacific basins are restricted to zones UC15d–UC17 (CC22– CC23), suggesting that sedimentation occurred between the late Campanian and early Maastrichtian. These biostratigraphic ages agree with previous age determinations, indicating that the upper Campanian–lower Maastrichtian deposits from both regions can be correlated. However, low-latitude calcareous nannofossils were particularly scarce in deposits drilled by the ANH-LA LOMA-1 core, likely owing to the influence of colder oceanic waters during the Maastrichtian.

CRediT authorship contribution statement

Estefanía Angulo-Pardo: Formal analysis, Conceptualization, Writing - original draft. **Felipe Vallejo-Hincapié:** Supervision, Conceptualization. **Rodrigo Do Monte Guerra:** Validation, Writing - review & editing. **Andrés Pardo-Trujillo:** Writing – review & editing, Supervision, Project administration. **Carlos A. Giraldo-Villegas:** Writing – original draft, Resources. **Jenny García González:** Resources. **Sebastian Hernández Duran:** Resources. **Sergio Herrera Quijano:** Resources. **Angelo Plata Torres:** Writing – review & editing, Validation. **Raúl Trejos-Tamayo:** Validation, Writing - review & editing.

Declaration of competing interest

The authors declare that they have no known competing financial interests or personal relationships that could have appeared to influence the work reported in this paper.

Data availability

Data will be made available on request.

Acknowledgments

This work was sponsored by the Agencia Nacional de Hidrocarburos and the Ministerio de Ciencia, Tecnología e Innovación, Colombia under Project Certificación de estratigrafía física y de edad de los núcleos de perforación recuperados por la Agencia Nacional de Hidrocarburos–ANH en las cuencas de Sinú-San Jacinto y Cordillera [contract FP44842-494-2017]. We would like to thank the Instituto de Investigaciones en Estratigrafía for providing the necessary work equipment and facilities. We are grateful to geologists German Eduardo Bonilla for providing some of the studied samples and Joan Sebastian Quintero for collaborating on the edition of the maps. Thanks to Sergio Celis for his field assistance. We also thank Dr. Mario Moreno and Dr. Andrea Concheyro for their helpful comments and suggestions, and Dr. Osman Varol for reviewing the manuscript.

Appendix A. Supplementary data

Supplementary data to this article can be found online at https://doi.org/10.1016/j.jsames.2023.104315.

Alphabetic list of calcareous nannofossils

Ahmuellerella octoradiata (Gorka, 1957) Reinhardt (1964)
Arkhangelskiella cymbiformis Vekshina (1959)
Braarudosphaera bigelowii (Gran and Braarud, 1935) Deflandre (1947)
Calculites obscurus (Deflandre, 1959) Prins and Sissingh in Sissingh (1977).
Ceratolithoides cf. C. *dongenii* Lees (2007)
Cribrocorona cf. C. *gallica* (Stradner, 1963) Perch-Nielsen (1973)
Cribrosphaerella circula (Risatti, 1973) Lees (2007)
Cribrosphaerella ehrenbergii (Arkhangelsky, 1912) Deflandre in Piveteau (1952)
Cyclagelosphaera margerelii Noël (1965)
Eiffellithus eximius (Stover, 1966) Perch-Nielsen (1968)
Eiffellithus parallelus Perch-Nielsen (1973)
Eiffellithus perch-nielseniae Shamrock in Shamrock and Watkins (2009)
Eiffellithus turriseiffelii (Deflandre in Deflandre and Fert, 1954) Reinhardt (1965)
Eprolithus cf. E. *moratus* (Stover, 1966).
Eprolithus floralis (Stradner, 1962) Stover (1966)
Gartnerago cf. G. *costatum* (Gartner, 1968) Bukry (1969)
Kamptnerius magnificus Deflandre (1959)
Lithastrinus grilli Stradner (1962)
Lithastrinus septenarius Forchheimer (1972)
Lithraphidites cf. L. *praequadratus* Roth (1978)
Manivitella pemmatoidea (Deflandre in Manivit, 1965) Thierstein (1971)
Microrhabdulus belgicus Hay and Towe (1963)
Microrhabdulus decoratus Defiandre (1959)
Microrhabdulus undosus Perch-Nielsen (1973)
Micula adumbrata Burnett (1997)
Micula concava (Stradner in Martini and Stradner, 1960) Verbeek (1976)
Micula cubiformis Forcbheimer (1972)
Micula staurophora (Gardet, 1955) Stradner (1963)
Micula swastica Stradner and Steinmetz (1984)
Octocyclus cf. O. *magnus* Black (1972)
Placozygus cf. P. *fibuliformis* (Reinhardt, 1964) Hoffmann (1970)
Prediscosphaera columnata (Stover, 1966) Perch-Nielsen (1984)
Prediscosphaera cretacea (Arkhangelsky, 1912) Gartner (1968)
Prediscosphaera spinosa (Bramlette and Martini, 1964) Gartner (1968)
Quadrum gartneri Prins and Perch-Nielsen in Manivit et al. (1977)
Reinhardtites anthoporus (Deflandre, 1959) Perch-Nielsen (1968)
Reinhardtites levis Prins Sissingh in Sissingh (1977).
Retecapsa angustiforata Black (1971)
Retecapsa crenulata (Bramlette and Martini, 1964) Grün in Grün and Allemann (1975)
Retecapsa surirella (Deflandre and Fert, 1954) Grün in Grün and Allemann (1975)
Rhagodiscus angustus (Stradner, 1963) Reinhardt (1971)
Staurolithites (Caratini, 1963).
Tetrapodorhabdus decorus (Deflandre in Deflandre and Fert, 1954) Wind and Wise in Wise and Wind (1977)
Uniplanarius gothicus (Deflandre, 1959).
Uniplanarius sissinghii (Perch-Nielsen, 1986) Farhan (1987)
Uniplanarius trifidus Stradner in Stradner and Papp (1961)
Watznaueria barnesae (Black in Black and Barnes, 1959) Perch-Nielsen (1968)
Watznaueria fossacincta (Black, 1971) Bown in Bown and Cooper (1989)
Zeugrhabdotus diplogrammus (Deflandre in Deflandre and Fert, 1954) Burnett in Gale et al. (1996)
Zeugrhabdotus embergeri (Noël, 1959) Perch-Nielsen (1984)
Zeugrhabdotus scutula (Bergen, 1994) Rutledge and Bown (1996)

References

Álvarez, E., González, H., 1978. Geología y geoquímica del Cuadrángulo I–7 (Urrao). Mapa escala 1:100.000. Ingeominas. Report 1761.
Barrantes, L.C., López, C., Patiño, A., Pinilla, A., Ramos, J.A., Ramos, K.G., Savanier, D., Orozco, L.A., 2019. Plancha 81–Puerto Libertador a Escala 1:100.000. Departamento de Córdoba. Servicio Geológico Colombiano, Explanatory Memory, p. 219.
Barrera, E., Savin, S.M., 1999. Evolution of Campanian–Maastrichtian marine climates and oceans. Spec. Pap. Geol. Soc. Am. 332, 245–282. https://doi.org/10.1130/0-8137-2332-9.245.
Barrero, 1979. Geology of the Central Western Cordillera, West of Buga and Roldanillo, Colombia, vol. 75. Ingeominas, Special Geological Publications.
Bayona, G., 2018. El inicio de la emergencia en los Andes del norte: una perspectiva a partir del registro tectónico-sedimentológico del Coniaciano al Paleoceno. Rev. Acad. Colomb. Cienc. Exactas Fis. Nat. 42, 364–378. https://doi.org/10.18257/raccefyn.632.
Bermúdez, H.D., García, J., Stinnesbeck, W., Keller, G., Rodríguez, J.V., Hanel, M., Hopp, J., Schwarz, W., Trieloff, M., Bolívar, L., Vega, F.J., 2016. The cretaceous Paleogene boundary at Gorgonilla Island, Colombia, South America. Terra. Nova 28, 83–90. https://doi.org/10.1111/ter.12196.
Bermúdez, H.D., Arenillas, I., Arz, J.A., Vajda, V., Renne, P.R., Gilabert, V., Rodríguez, J. V., 2019. The cretaceous/paleogene boundary deposits on Gorgonilla Island. In: Gómez, J., Mateus–Zabala, D. (Eds.), The Geology of Colombia, Volume 3 Paleogene–Neogene, vol. 37. Servicio Geológico Colombiano, Special Geological Publications, p. 19. https://doi.org/10.32685/pub.esp.37.2019.01.
Botero-García, M., Vinasco, C.J., Restrepo-Moreno, S.A., Foster, D., Kamenov, G.D., 2023. Caribbean–South America interactions since the late cretaceous: insights from zircon U-Pb and Lu-Hf isotopic data in sedimentary sequences of the northwestern andes. J. S. Am. Earth Sci. 123, 104231 https://doi.org/10.1016/j.jsames.2023.104231.
Bown, P.R., Young, J.R., 1997. Mesozoic calcareous nannoplankton classification. J. Nannoplankt. Res. 19, 21–36.
Bown, P.R., Young, J.R., 1998. Introduction–calcareous nannoplankton biology. In: Bown, P.R. (Ed.), Calcareous Nannofossils Biostratigraphy. British Micropalaeontological Society Publications Series, Kluwer Academic Publishers, London, pp. 1–15.
Bralower, T.J., Mark, R., Sliter, W.V., Thierstein, H.R., 1995. An Integrated Cretaceous Microfossil Biostratigraphy, vol. 54. Society for Sedimentary Geology, Special Publications, pp. 65–79. https://doi.org/10.2110/pec.95.04.0065.
Buchs, D.M., Kerr, A.C., Brims, J.C., Zapata-Villada, J.P., Correa-Restrepo, T., Rodríguez, G., 2018. Evidence for subaerial development of the Caribbean oceanic plateau in the Late Cretaceous and palaeo-environmental implications. Earth Planet Sci. Lett. 499, 62–73. https://doi.org/10.1016/j.epsl.2018.07.020.
Bürgl, H., 1961. Geología de los alrededores de Ortega, Tolima. Bol. Geol. 8, 21–38.
Bürgl, H., Dumit, Y., 1954. El Cretáceo Superior en la región de Girardot. Bol.Geol.Serv. Geol. Nac. 2, 23–48. https://doi.org/10.32685/0120-1425/bolgeol2.1.1954.350.
Burnett, J.A., 1998. Upper cretaceous. In: Bown, P.R. (Ed.), Calcareous Nannofossils Biostratigraphy. British Micropalaeontological Society Series, Chapman and Hall/Kluwer Academic Publishers, London, pp. 132–199.
Chenevart, C., 1963. Les dorsales transverses anciennes de Colombie et leurs homologue dÁmerique Latine. Eclogae Geol. Helv. 56, 907–927.
Clavijo, T.J., Barrera, O.R., 2001. Geología de las planchas 44 Sincelejo y 52 Sahagún. In: Escala 1:100.000, vol. 63. Ingeominas. Explanatory Memory.

Concheyro, G.A., 1995. Nanofósiles calcáreos del Cretácico Superior y Paleógeno de Patagonia, Argentina. Doctoral thesis, vol. 158. Faculty de Ciencias Exactas y Naturales, Universidad de Buenos Aires.
Cunha, A.S., Antunes, R.L., Burnett, J.A., 1997. Calcareous nannofossils and the Santonian/Campanian and Campanian/Maastrichtian boundaries on the Brazilian Continental Margin: historical overview and state of the art. Cretac. Res. 18, 823–832. https://doi.org/10.1006/cres.1997.0089.
De Romero, L.M., Truskowski, I.M., Bralower, T.J., Bergen, J.A., Odreman, O., Zachos, J. C., Galea-Alvarez, F.A., 2003. An integrated calcareous microfossil biostratigraphic and carbon-isotope stratigraphic framework for the La Luna Formation, western Venezuela. Palaios 18, 349–366. https://doi.org/10.1669/0883-1351(2003)018<0349:AICMBA>2.0.CO;2.
Diaz, L., 1994. Reconstruction de la Cuenca del Valle Superior del Magdalena, a finales del Cretácico. In: Etayo, F. (Ed.), Estudios Geológicos del Valle Superior del Magdalena. Universidad Nacional de Colombia, Bogotá. XI-1-XI-13.
Díaz-Cañas, J.S., Patarroyo, P., 2014. Upper campanian - lower maastrichtian pachydiscus from the Penderisco Formation, western Cordillera (antioquia - Colombia). Geol. Colomb. 39, 15–21.
Dubicka, Z., Jurkowska, A., Thibault, N., Razmjooei, M.J., Razmjooei, M.J., Wójcik, K., Gorzelak, P., Felisiak, I., 2017. An integrated stratigraphic study across the Santonian/Campanian boundary at Bocieniec, southern Poland: a new boundary stratotype candidate. Cretac. Res. 80, 61–85. https://doi.org/10.1016/j.cretres.2017.07.012.
Dueñas, J.H., 1989. Asociaciones palinológicas de las formaciones colon y molino Nor. Oriente colombiano, vol. 7. Paleobotânica e Palinologia na América do Sul, Special Publication, pp. 173–181. https://doi.org/10.11606/issn.2317-8078.v0i7p173-181.
Dueñas, H., Gómez, C., 2013. Bioestratigrafía de la Formación Cansona en la Quebrada Peñitas, Cinturón de San Jacinto. Implicaciones paleogeográficas. Rev. Acad. Colomb. Cienc. Exactas Fis. Nat. 37, 527–539. https://doi.org/10.18257/raccefyn.33.
Duque-Caro, H., 1967a. Observaciones generales a la bioestratigrafía y geología regional en los departamentos de Bolívar y Córdoba, vol. 24. Boletín Geológico de la Universidad Industrial de Santander, pp. 71–87.
Duque-Caro, H., 1967b. Informe Bioestratigráfico Preliminar Cuadrángulos E-8 Y D-8, vol. 30. Servicio Geológico Nacional.
Duque-Caro, H., 1972a. Ciclos tectónicos y sedimentarios en el Norte de Colombia y sus relaciones con la paleoecología. Bol. Geol. 19, 1–23. https://doi.org/10.32685/0120-1425/bolgeol19.3.1971.401.
Duque-Caro, H., 1972b. Relaciones entre la bioestratigrafía y la cronoestratigrafia en el llamado geosinclinal de Bolívar. Bol. Geol. 19, 25–68. https://doi.org/10.32685/0120-1425/bolgeol19.3.1971.403.
Duque-Caro, H., 1973. Guidebook to the Geology of the Monteria Area, vol. 49. Colombian Society of Petroleum Geologists and Geophysicists.
Duque-Caro, H., 1978. Geotectónica y evolución de la región Noroccidental Colombiana. Bol. Geol. 23, 4–37. https://doi.org/10.32685/0120-1425/bolgeol23.3.1980.257.
Duque-Caro, H., 1979. Major structural elements and evolution of the northwestern Colombia. In: Watkins, L.S., Montadcrt, L., Dickerson, P.W. (Eds.), Geological and Geophysical Investigations of Continental Margins, vol. 29. American Association of Petroleum Geologists, Memories, pp. 329–351.
Duque-Caro, H., 1984. Estilo extructural, diaprimismo y espisodios de acrecimiento del terreno Sinú-San Jacinto en el NW de Colombia. Bol. Geol. 27, 1–29.
Duque-Caro, H., 1990. El bloque del Chocó en el noroccidente suramericano: implicaciones estructurales, tectonoestratigráficas y paleogeográficas. Bol. Geol. 31, 48–71. https://doi.org/10.32685/0120-1425/bolgeol31.1.1990.179.
Duque-Caro, H., Dueñas, H., 1987. The stratigraphy and diapiric structures of the Northwestern Colombia (Cartagena-Carmen de Bolívar áreas). In: Colombian Association of Petroleum Geology and Geophysics. 25th Field Conference, pp. 283–303.
Echeverri, S., Cardona, A., Pardo-Trujillo, A., Borrero, C., Rosero, S., López, S., 2015. Correlación y geocronología Ar-Ar del basamento Cretácico y el relleno sedimentario Eoceno superior-Mioceno (Aquitaniano inferior) de la cuenca de antearco de Tumaco, SW de Colombia. Rev. Mex. Ciencias Geol. 32, 179–189.
Erlich, R.N., Nederbragt, A.J., Lorente, M.A., 2000. Birth and death of the late cretaceous "La Luna Sea", and origin of the tres esquinas phosphorites. J. S. Am. Earth Sci. 13, 21–45. https://doi.org/10.1016/S0895-9811(00)00016-X.
Etayo-Serna, F., 1979. Zonation of the cretaceous of central Colombia by ammonites. Ingeominas. Special. Geol. Publ. 2, 1–186.
Etayo-Serna, F., 1985. *Trochoceramus* del Campaniano-Maastrichtiano en la Formación Espinal de la Cordillera Occidental de Colombia. Geol. Norandina 9, 27–30.
Etayo-Serna, F., 1989. Campanian to maastrichtian fossils in the northeastern western Cordillera, Colombia. Geol. Norandina 11, 23–32.
Etayo-Serna, F., 1994. Estudios Geológicos del Valle Superior del Magdalena. Special Publication, Universidad Nacional de Colombia, Bogotá, p. 359.
Etayo, F., Renzoni, G., Barrero, D., 1969. Contornos sucesivos del mar Cretácico en Colombia. In: Etayo, F., Cáceres, C. (Eds.), Memorias Primer Congreso Colombiano de Geología, Bogotá, pp. 217–252.
Etayo-Serna, F., Parra, E., Rodríguez, G., 1982. Análisis facial del "Grupo Dagua" con base en secciones aflorantes al oeste de Toro (Valle del Cauca). Geol. Norandina 5, 3–12.
Fabre, A., 1985. Dinámica de la sedimentación Cretácica en la región de la Sierra Nevada del Cocuy (Cordillera Oriental de Colombia). In: Etayo-Serna, F., Laverde-Montaño, F. (Eds.), Proyecto Cretácico, vol. 16. Ingeominas, Special Geological Publications, Bogotá, p. 20.
Föllmi, K.B., Garrison, R.E., Ramírez, P.C., Zambrano Ortiz, F., Kennedy, W.J., Lehner, B. L., 1992. Cyclic phosphate–rich successions in the Upper Cretaceous of Colombia. Palaeogeogr. Palaeoclimatol. Palaeoecol. 93, 151–182. https://doi.org/10.1016/0031-0182(92)90095-M.
Gandolfi, R., 1955. The genus Globotruncana in northeastern Colombia. Bull. Am. Paleontol. 30, 1–20.
Garzon, S., Warny, S., Bart, P.J., 2012. A palynological and sequence-stratigraphic study of Santonian–Maastrichtian strata from the Upper Magdalena Valley basin in central Colombia. Palynology 36, 112–133. https://doi.org/10.1080/01916122.2012.675147.
Geotec, 1997. Cartografía geológica de la Región del Sinú (Noroeste de Colombia) (Planchas 50, 51, 59, 60, 61, 69, 70, 71, 79 y 80). Ingeominas, p. 3. Tech. Rep.
Geotec, 2003. Geología de Los Cinturones Sinú - San Jacinto, Escala 1:100.000. Ingeominas, p. 135. Explanatory Memory.
Gómez-Cruz, A., Moreno-Sánchez, M., Pardo-Trujillo, A., 2002. Afloramientos fosilíferos del Cretáceo Superior en el municipio de Pijao (borde Occidental de la Cordillera Central, Colombia). Geo. Eco. Trop 26, 41–50.
Giraldo-Villegas, C.A., Rodríguez-Tovar, F.J., Celis, S.A., Pardo-Trujillo, A., Duque-Castaño, M.L., 2023. Paleoenvironmental conditions over the caribbean large igneous province during the late cretaceous in NW of South American margin: a sedimentological and ichnological approach. Cretac. Res. 142, 105407 https://doi.org/10.1016/j.cretres.2022.105407.
Gómez, E., Jordan, T., Almandiger, R., Hegarty, K., Kelly, S., Heizler, M., 2003. Controls on architecture of the late cretaceous to cenozoic southern middle Magdalena Valley Basin, Colombia. The Geolical Society of America, GSA Bulletin 115, 131–147. https://doi.org/10.1130/0016-7606(2003)115<0131:COAOTL>2.0.CO;2.
Guerra, R.M., Concheyro, A., Wise, S.W., Fauth, G., 2016. Late campanian-maastrichtian Kamptnerius magnificus acme in the South atlantic section of the Southern ocean, ODP holes 690C and 700B. Micropaleontology 62, 213–219.
Guerrero, J., Sarmiento, G., Navarrete, R., 2000. The stratigraphy of the W side of the cretaceous Colombian basin in the upper Magdalena Valley. Reevaluation of selected areas and type localities including aipe, guaduas, ortega, and piedras. Geol. Colomb. 25, 45–110.
Guerrero, J., Montes, L., Jaillard, E., Kammer, A., 2021. Seismic interpretation of the cretaceous unconformities and sequences in the middle Magdalena Valley and the western margin of the eastern Cordillera, Colombia. Comptes Rendus 353, 155–172.
Guzmán, G., 2007. Stratigraphy and Sedimentary Environment and Implications in the Plato Basin and the San Jacinto Belt, Northwestern Colombia. Doctoral thesis, University of Liege, p. 487.
Guzmán, G., Clavijo, J., Barrera, R., 1994. Geología Bloque Santero, Secciones Estratigráficas. Ingeominas, Unpublished report, p. 135.
Guzmán, G., Gómez, E., Serrano, B., 2004. Geología de los Cinturones del Sinú, San Jacinto y borde Occidental del Valle Inferior del Magdalena, Caribe Colombiano. Escala 1:300.000. Ingeominas, p. 133. Explanatory Memory.
Haq, B.U., 2014. Cretaceous eustasy revisited. Global Planet. Change 113, 44–58. https://doi.org/10.1016/j.gloplacha.2013.12.007.
Hernández, S., 2021. Litogeoquímica de las unidades del Cretácico Superior, su relación con las áreas de aporte y evolución de los medios sedimentarios, Cuenca del Valle Superior del Magdalena, Colombia. Master thesis Facultad de Ciencias. Universidad Nacional de Colombia 226.
Herrera, J., Bermúdez, H., Alfonso, M., Calderon, J., Pardo, A., Lozano, A., 2009. Cartografía Geológica de un área del Cinturón Plegado de San Jacinto. X Simposio Bolivariano Exploración Petrolera, vol. 10. Cuencas Subandinas held, Cartagena.
Iturralde-Vinent, M.A., 2005. La Paleogeografía del Caribe y sus implicaciones para la biogeografía histórica. Revista del Jardín Botánico Nacional, pp. 49–78.
Jaramillo, C., Yepes, O., 1994. Palinoestratigrafía del Grupo Oliní (Coniaciano-Campaniano), Valle Superior del Magdalena, Colombia. In: Etayo, F. (Ed.), Estudios geológicos del Valle Superior del Magdalena, vol. 17. Universidad Nacional de Colombia, Bogotá, pp. 1–17.
Jelby, M.E., Thibault, N., Surlyk, F., Ullmann, C.V., Harlou, R., Korte, C., 2014. The lower Maastrichtian Hvidskud succession, Møns Klint, Denmark: calcareous nannofossils biostratigraphy, carbon isotope stratigraphy, and bulk and brachiopod oxygen isotopes. Bull. Geol. Soc. Den. 62, 89–104.
Kerr, A.C., Tarney, J., 2005. Tectonic evolution of the Caribbean and northwestern South America: the case for accretion of two Late Cretaceous oceanic plateaus. Geology 33, 269–272. https://doi.org/10.1130/G21109.1.
Kita, Z.A., Watkins, D.K., Sageman, B., 2017. High-resolution calcareous nannofossils biostratigraphy of the santonian/campanian stage boundary, western interior basin, USA. Cretac. Res. 69, 49–55. https://doi.org/10.1016/j.cretres.2016.08.015.
Lamolda, M.A., Paul, C.R.C., Peryt, D., Pons, J.M., 2014. The global boundary stratotype and section point (GSSP) for the base of the santonian stage, "cantera de Margas", olazagutia, northern Spain. Episodes 37, 2–13. https://doi.org/10.18814/epiiugs/2014/v37i1/001.
Lees, J.A., 2002. Calcareous nannofossils biogeography illustrates palaeoclimate change in the late cretaceous Indian ocean. Cretac. Res. 23, 537–634. https://doi.org/10.1006/cres.2003.1021.
Linnert, C., Robinson, S.A., Lees, J.A., Bown, P.R., Pérez-Rodríguez, I., Petrizzo, M.R., Falzoni, F., Littler, K., Arz, J.A., Russell, E.E., 2014. Evidence for global cooling in the late cretaceous. Nat. Commun. 5, 4194. https://doi.org/10.1038/ncomms5194.
Mann, P., 1999. Caribbean sedimentary basins: classification and tectonic setting from Jurassic to present. In: Mann, P. (Ed.), Caribbean Basins. Sedimentary Basins of the World, Amsterdam, pp. 3–31. https://doi.org/10.1016/S1874-5997(99)80035-5.
Mann, P., Escalona, A., Castillo, M.V., 2006. Regional geologic and tectonic setting of the Maracaibo supergiant basin, western Venezuela. Am. Assoc. Petrol. Geol. Bull. 90, 445–477. https://doi.org/10.1306/10110505031.
Martínez, J.I., 1989. Foraminiferal Biostratigraphy and Paleoenvironments of the Maastrichtian Colon Mudstones of Northern South America, vol. 35. The Micropaleontology project, Inc., pp. 97–113

Martínez, J.I., 2003. The paleoecology of Late Cretaceous upwelling events from the upper Magdalena Basin, Colombia. Palaios 18, 305–320. https://doi.org/10.1669/0883-1351(2003)018<0305:TPOLCU>2.0.CO;2.

Martínez, J.I., Hernández, R., 1992. Evolution and drowning of the Late Cretaceous Venezuelan carbonate platform. J. S. Am. Earth Sci. 5, 197–210. https://doi.org/10.1016/0895-9811(92)90038-Z.

Miniati, F., Petrizzo, M.R., Falzoni, F., Erba, E., 2020. Calcareous plankton biostratigraphy of the Santonian-Campanian boundary interval in the Bottaccione section (Umbria-Marche basin, central Italy). Riv. Ital. Paleontol. Stratigr. 126, 783–801. https://doi.org/10.13130/2039-4942/14399.

Moore, B.R., 2016. Santonian-Campanian Calcareous Nannofossils Paleobiogeography. Master Thesis. Department of Earth and Atmospheric Sciences, University of Nebraska, p. 84.

Mora, J.A., Oncken, O., Le Breton, E., Ibánez-Mejia, M., Faccenna, C., Veloza, G., Vélez, V., Freitas, M., Mesa, A., 2017. Linking late cretaceous to eocene tectonostratigraphy of the san Jacinto fold belt of NW Colombia with caribbean plateau collision and flat subduction. Tectonics 36, 2599–2629. https://doi.org/10.1002/2017TC004612.

Moreno-Sánchez, M., Pardo-Trujillo, A., Gómez, A.J., 2002. Ambientes oceánicos someros en Puente Umbría (Cordillera Occidental, Colombia) durante el Campaniano-Maastrichtiano. Geo. Eco. Trop 26, 75–90.

Moreno-Sánchez, M., Pardo-Trujillo, A., 2003. Stratigraphical and sedimentological constraints on western Colombia: implications on the evolution of the Caribbean plate. In: Bartolini, C., Buffler, R.T., Blickwede, J. (Eds.), The Circum-Gulf of Mexico and the Caribbean: Hydrocarbon Habitats, Basin Formation, and Plate Tectonics: American Association of Petroleum Geologists, Memoir, vol. 79, pp. 891–924. https://doi.org/10.1306/M79877C40.

Navarrete-Parra, R.E., Parra, F.J., Pérez, P.J., Daza, D., Sánchez, C., Prince, M., Rodriguez, M., 2018. Turonian-campanian foraminifera zonation for the La Luna and lower Umir formations, middle Magdalena Valley Basin, northern Colombia. In: Cusminsky, G.C., Bernasconi, E., Concheyro, G.A. (Eds.), Advances in South American Micropaleontology. Springer Earth System Sciences, pp. 67–114. https://doi.org/10.1007/978-3-030-02119-1_4.

Nivia, Á., 1996. The Bolivar mafic-ultramafic complex, SW Colombia: the base of an obducted plateau. J. S. Am. Earth Sci. 9, 59–68. https://doi.org/10.1016/0895-9811(96)00027-2.

O'Brien, C.L., Robinson, S.A., Pancost, R.D., Damste, J.S.S., Schouten, S., Lunt, D.J., Alsenz, H., Bornemann, A., Bottini, C., Brassell, S.C., Farnsworth, A., Forster, A., Huber, B.T., Inglis, G.N., Jenkyns, H.C., Linnert, C., Littler, K., Markwick, P., McAnenao, A., Mutterlose, J., Naafs, D.A., Püttmann, W., Sluijs, A., van Helmond, N. A.G.M., Vellekoop, J., Wagner, T., Wrobel, N.E., 2017. Cretaceous sea-surface temperature evolution: constraints from TEX86 and planktonic foraminiferal oxygen isotopes. Earth Sci. Rev. 172, 224–247. https://doi.org/10.1016/j.earscirev.2017.07.012.

Odin, G.S., 2001. The Campanian-Maastrichtian stage boundary: characterisation at Tercis les Bains (France) and correlation with Europe and other continents. In: Odin, G.S. (Ed.), Developments in Palaeontology and Stratigraphy, vol. 36. International Union of Geological Sciences, special publication, pp. 805–819. https://doi.org/10.1016/S0920-5446(01)80070-4.

Odin, G.S., Lamaurelle, M.A., 2001. The global Campanian-Maastrichtian stage boundary. Int. Union Geol. Sci. 24, 229–238. https://doi.org/10.18814/epiiugs/2001/v24i4/002. Episodes.

Páez-Reyes, M., Carvajal-Ortiz, H., Sahoo, S.K., Varol, O., Miller, B.V., Hughes, G.W., Gaona-Narvaez, T., Patarroyo, G.D., Curtis, J.H., Lerma, I., Copeland, P., 2021. Assessing the contribution of the La Luna Sea to the global sink of organic carbon during the cenomanian-turonian oceanic anoxic event 2 (OAE2). Global Planet. Change 199, 103424. https://doi.org/10.1016/j.gloplacha.2021.103424.

Pardo-Trujillo, A., Moreno-Sánchez, M., Gómez, A., 2002a. Estratigrafía y facies del Cretáceo Superior-Terciario Inferior (?) en el sector de Nogales-Monteloro (borde Occidental de la Cordillera Central, Colombia). Geo. Eco. Trop 26, 9–40.

Pardo-Trujillo, A., Moreno-Sánchez, M., Gómez, A., 2002b. Estratigrafía y análisis facial del Cretácico Superior en el sector de Apia-Pueblo Rico (Cordillera Occidental, Colombia). Geo-Eco-Trop 26, 51–74.

Pardo-Trujillo, A., Cardona, A., Giraldo, A.S., León, S., Vallejo, F., Trejos-Tamayo, R., Plata, A., Ceballos, J., Echeverri, S., Barbosa-Espitia, A., Slattery, J., Salazar-Ríos, A., Botello, G.E., Celis, S.A., Osorio-Granada, E., Giraldo-Villegas, C.A., 2020. Sedimentary record of the Cretaceous-Paleocene arc-continent collision in the northwestern Colombian Andes: insights from stratigraphic and provenance constraints. Sediment. Geol. 401, 105627 https://doi.org/10.1016/j.sedgeo.2020.105627.

Patarroyo, P., 2011. Sucesión de amonitas del Cretácico Superior (Cenomaniano–Coniaciano) de la parte más alta de la Formación Hondita y de la Formación Loma Gorda en la Quebrada Bambucá, Aipe-Huila (Colombia, S. A.). Bol. Geol. 33, 69–92.

Patarroyo, P., Bengtson, P., 2017. *Codazziceras ospinae* (karsten, 1858) from the turonian (upper cretaceous) of Colombia. Cretac. Res. 88, 392–398. https://doi.org/10.1016/j.cretres.2017.04.002.

Patarroyo, G.D., Torres, G.A., Rincón, D.A., Cárdenas, C.P., Márquez, R.E., 2017. Bioestratigrafía e inferencias paleoambientales de las asociaciones de foraminíferos en las Formaciones Cretácicas La Luna-Colón (cuenca del Catatumbo, Colombia). Bol. Geol. 39, 25–40. https://doi.org/10.18273/revbol.v39n3-2017002.

Patarroyo, G.D., Kochhann, K.G.D., Ceolin, D., Guerra, R., Laila, A., Bom, M.H.H., 2022. Paleoenvironmental changes recorded at a late Maastrichtian marine succession of northern South America. J. S. Am. Earth Sci., 104015 https://doi.org/10.1016/j.jsames.2022.104015.

Patiño, A., Pinilla, A., Cristancho, A., Ibáñez, R.P., Savanier, D., Orozco, L.A., Gómez, C. D., López, C., Quiñonez, C.S., Ramos, J.A., Gil, C.A., Ramos, K.G., Román, J.A., 2019. Plancha 91–Belencito a escala 1:100.000. Departamento de Córdoba y Antioquia. Servicio Geológico Colombiano, p. 241. Explanatory Memory.

Perch-Nielsen, K., 1985. Mesozoic calcareous nannofossils. In: Bolli, H.M., Saunders, J.B., Perch-Nielsen, K. (Eds.), Plankton Stratigraphy. Cambridge University Press, Cambridge, pp. 329–426.

Pérez, J.P.P., Parra, F.J., Navarrete, R.E., Sánchez, C., Daza, D., Rodriguez, M., Prince, M., 2018. Turonian–santonian calcareous nannofossils biozonation for La Luna Formation, middle Magdalena Valley Basin, northern Colombia. In: Cusminsky, G.C., Bernasconi, E., Concheyro, G.A. (Eds.), Advances in South American Micropaleontology. Springer Earth System Sciences, pp. 46–66. https://doi.org/10.1007/978-3-030-02119-1_3.

Petters, V., 1955. Development of upper cretaceous foraminiferal faunas in Colombia. J. Paleontol. 29, 212–225.

Renne, P.R., Arenillas, I., Arz, J.A., Vajda, V., Gilabert, V., Bermúdez, H.D., 2018. Multi-proxy Record of the Chicxulub Impact at the Cretaceous-Paleogene Boundary from Gorgonilla Island, Colombia, vol. 46. The Geological Society of America, pp. 547–550. https://doi.org/10.1130/G40224.1.

Rodríguez, G., Arango, M., 2013. Formación Barroso: arco volcánico toleitico y diabasas de San José de Urama: un prisma acrecionario T-MORB en el segmento norte de la Cordillera Occidental de Colombia. Boletín Ciencias de la Tierra 33, 17–38.

Roth, P.H., 1978. Cretaceous Nannoplankton Biostratigraphy and Oceanography of the Northwestern Atlantic Ocean, vol. 44. Deep Sea Drilling Project, pp. 731–759. Initial Reports.

Roth, P.H., Thierstein, H., 1972. Calcareous nannoplankton: leg 14 of the deep sea drilling project. Deep Sea Drilling Project 14, 421–485. https://doi.org/10.2973/dsdp.proc.14.114.1972. Initial report.

Sarmiento, L.F., 2018. Cretaceous Stratigraphy and paleo-facies maps of northwestern South America. In: Cediel, F., Shaw, R.P. (Eds.), Geology and Tectonics of Northwestern South America. Frontiers in Earth Sciences, pp. 673–747. https://doi.org/10.1007/978-3-319-76132-9_10.

Sheldon, E., Ineson, J., Bown, P., 2010. Late maastrichtian warming in the boreal realm: calcareous nannofossils evidence from Denmark. Palaeogeogr. Palaeoclimatol. Palaeoecol. 295, 55–75. https://doi.org/10.1016/j.palaeo.2010.05.016.

Sissingh, W., 1977. Biostratigraphy of Cretaceous calcareous nannoplankton. Geol. Mijnbouw 56, 37–65.

Sissingh, W., 1978. Microfossil biostratigraphy and stage-stratotypes of the Cretaceous. Geol. Mijnbouw 57, 433–440.

Solé de Porta, N.S., 1972. Palinología de la Formación Cimarrona (Maastrichtiense) en el Valle Medio del Magdalena, Colombia. Stud. Geol. Salmant. 4, 103–142.

Spikings, R., Cochrane, R., Villagomez, D., Van der Lelij, R., Vallejo, C., Winkler, W., Beate, B., 2015. The geological history of northwestern South America: from pangaea to the early collision of the caribbean large igneous province (290–75Ma). Gondwana Res. 27, 95–139. https://doi.org/10.1016/j.gr.2014.06.004.

Talukdar, S., Marcano, F., 1994. Petroleum system of the maracaibo basin, Venezuela. In: Magoon, L.B., Dow, W.G. (Eds.), The Petroleum System-From Source to Trap. American Association of Petroleum Geologists, Memoir, pp. 463–481. https://doi.org/10.1306/M60585C29.

Tchegliakova, N., Mojica, J., 2001. El Senoniano de la Barrera de Girardot-Guataqui, Valle alto del Magdalena, Colombia: precisiones sobre la estratigrafia y establecimiento de una zonacion micropaleontologica. Rev. Acad. Colomb. Ciencias Exactas, Fis. Nat. 25, 37–75.

Terraza-Melo, R., Caicedo, A.J.C., Jiménez, D.M., Morales, C.J., 2002. Geología de la plancha 264 Espinal, Escala 1:100.000, vol. 128. Ingeominas, Explanatory Memory.

Théry, J.M., 1980. Evolution géotectonique de l'Occident colombien, nouvelles données. Bull. Cent. Rech. Explor.-Prod. Elf-Aquitaine 4, 649–660.

Thibault, N., Gardin, S., 2006. Maastrichtian calcareous nannofossils biostratigraphy and palaeoecology in the equatorial atlantic (demerera rise, ODP leg 207 hole 1258A). Rev. Micropaleontol. 49, 199–214. https://doi.org/10.1016/j.revmic.2006.08.002.

Thibault, N., Gardin, S., 2007. The late Maastrichtian nannofossils record of climate change in the South Atlantic DSDP Hole 525A. Mar. Micropaleontol. 65, 163–184. https://doi.org/10.1016/j.marmicro.2007.07.004.

Thibault, N., Galbrun, B., Gardin, S., Minoletti, F., Le Callonnec, L., 2015a. The end-Cretaceous in the southwestern Tethys (Elles, Tunisia): orbital calibration of paleoenvironmental events before the mass extinction. Int. J. Earth Sci. 105, 771–795. https://doi.org/10.1007/s00531-015-1192-0.

Thibault, N., Anderskouv, K., Bjerager, M., Boldreel, L.O., Jelby, M.E., Stemmerik, L., Surlyk, F., 2015b. Upper Campanian–Maastrichtian chronostratigraphy of the Skælskør-1 core, Denmark: correlation at the basinal and global scale and implications for changes in sea-surface temperatures. Lethaia 48, 549–560. https://doi.org/10.1111/let.12128.

Thibault, N., Harlou, R., Schovsbo, N.H., Stemmerik, L., Surlyk, F., 2016. Late cretaceous (late campanian–maastrichtian) sea-surface temperature record of the boreal chalk sea. Clim. Past 12, 429–438. https://doi.org/10.5194/cp-12-429-2016.

Thierstein, H.R., 1981. Late Cretaceous Nannoplankton and the Change at the Cretaceous- Tertiary Boundary, vol. 32. Deep Sea Drilling Project, Special Publication, pp. 355–394.

Ucaldas-Minciencias-Anh, 2020. Análisis de facies y paleo-ambientes de depósito para los pozos perforados en las cuencas de Cesar Ranchería y Valle Medio del Magdalena. Unpublished report, p. 100.

Universidad de Caldas, 2012. Cartografía a escala 1:100.000 y estratigrafía de un sector de la cuenca Tumaco, perforación de pozos tipo Slim hole y análisis de pozos Chaguí-1 y Remolino Grande -1, p. 30. Unpublished report.

Vergara, S.L., 1994. Stratigraphic, micropaleontologic and organic geochemical relations in the cretaceous of the upper Magdalena Valley, Colombia. Doctoral thesis Fachbereich Geowissenschften und Geographie, University of Giessen 240.

Vergara, S.L., 1997. Paleontological notes on some foraminifera from the cretaceous of the upper Magdalena Valley, Colombia. Geol. Colomb. 22, 121–133.

Villagómez, D., Spikings, R., Magna, T., Kammer, A., Winkler, W., Beltrán, A., 2011. Geochronology, geochemistry and tectonic evolution of the western and central cordilleras of Colombia. Lithos 125, 875–896. https://doi.org/10.1016/j.lithos.2011.05.003.

Villagómez, D., Spikings, R., 2013. Thermochronology and tectonics of the central and western cordilleras of Colombia. Early Cretaceous-Tertiary evolution of the northern Andes 160, 228–249. https://doi.org/10.1016/j.lithos.2012.12.008.

Villamil, T., 1998. Chronology, relative sea-level history and a new sequence stratigraphic model for basinal Cretaceous of Colombia. In: Pindell, J., Drake, C. (Eds.), Eustacy and Tectonostratigraphic Evolution of Northern South America, vol. 58. Society for Sedimentary Geology, Special Publication, pp. 161–216. https://doi.org/10.2110/pec.98.58.0161.

Villamil, T., Arango, C., Hay, W.W., 1999. Plate tectonic paleoceanographic hypothesis for Cretaceous source rocks and cherts of northern South America. Geol. Soc. Am. Spec. Pap. 332, 191–202. https://doi.org/10.1130/0-8137-2332-9.191.

Villamil, T., Arango, C., 1998. Integrated stratigraphy of latest Cenomanian and early Turonian facies of Colombia. In: Pindell, J., Drake, C. (Eds.), Eustacy and Tectonostratigraphic Evolution of Northern South America. Society for Sedimentary Geology, Special Publication, Tulsa, pp. 129–159. https://doi.org/10.2110/pec.98.58.0129.

Voigt, S., Gale, A.S., Jung, C., Jenkyns, H.C., 2012. Global correlation of Upper Campanian - Maastrichtian successions using carbon-isotope stratigraphy: development of a new Maastrichtian timescale. Newsl. Stratigr. 45, 25–53. https://doi.org/10.1127/0078-0421/2012/0016.

Walaszczyk, I., Čech, S., Crampton, J.S., Dubicka, Z., Ifrim, C., Jarvis, I., Kennedy, W.J., Lees, J.A., Lodowski, D., Pearce, M., Uličný, D., Peryt, D., Voigt, S., Sageman, B.B., Wiese, F., Schiøler, P., Todes, J., 2021. The global boundary stratotype section and point (GSSP) for the base of the coniacian stage (Salzgitter-Salder, Germany) and its auxiliary sections (słupia nadbrzeżna, central Poland; střeleč, Czech republic; and el rosario, NE Mexico). Int. Union Geol. Sci. 1–40 Episodes 45, 181–220.

Watkins, D.K., Wise Jr., S.W., Popsichal, J.J., Crux, J., 1996. Upper Cretaceous calcareous nannofossils biostratigraphy and paleoceanography of the Southern Ocean. Pap. Earth Atmos. Sci. 258, 355–381.

Weber, M., Gómez, J., Cardona, A., Duarte, E., Pardo–Trujillo, A., Valencia, V.A., 2015. Geochemistry of the Santa fé batholith and buriticá tonalite in NW Colombia-evidence of subduction initiation beneath the Colombian caribbean plateau. J. S. Am. Earth Sci. 62, 257–274. https://doi.org/10.1016/j.jsames.2015.04.002.

Wolfgring, E., Wagreich, M., Dinarès-Turell, J., Gier, S., Böhm, K., Sames, B., Spötl, C., Popp, F., 2018. The Santonian–Campanian boundary and the end of the Long Cretaceous Normal Polarity–Chron: isotope and plankton stratigraphy of a pelagic reference section in the NW Tethys (Austria). Newsl. Stratigr. 51, 445–476. https://doi.org/10.1127/nos/2018/0392.

Yepes, O., 2001. Maastrichtian-Danian dinoflagellate cyst biostratigraphy and biogeography from two equatorial sections in Colombia and Venezuela. Palynology 25, 217–249. https://doi.org/10.1080/01916122.2001.9989561.

Zapata-Villada, J., Restrepo, J., Cardona, A., Martens, U., 2017. Geoquímica y geocronología de las rocas volcánicas básicas y el gabro de Altamira, Cordillera Occidental (Colombia): registro de ambientes de Plateau y arco oceánico superpuestos durante el Cretácico. Bol. Geol. 39, 13–30. https://doi.org/10.18273/revbol.v39n2-20170017.

Zapata-Villada, J.P., Cardona, A., Serna, S., Rodíguez, G., 2021. Late Cretaceous to Paleocene magmatic record of the transition between collision and subduction in the Western and Central Cordillera of northern Colombia. J. S. Am. Earth Sci. 112, 103557. https://doi.org/10.1016/j.jsames.2021.103557.